

学位論文 (要約)

Photo-induced magnetization of a two-dimensional  
cobalt–octacyanidotungstate bimetal assembly

(二次元コバルト–オクタシアノタングステン  
錯体の光磁性現象)

平成 28 年 12 月博士 (理学) 申請

東京大学大学院理学系研究科

化学専攻

宮本 靖人

# Abstract

---

## Introduction

Photo-induced phase transitions have been intensively studied as one of the attractive issues of non-equilibrium phenomena. Several types of materials exhibiting photo-induced phase transition have been reported up to date, for example, chalcogenides, metal oxides, spin-crossover complexes, and cyanide-bridged bimetal assemblies. Cobalt–octacyanidotungstate bimetal assemblies have been reported to show photo-induced magnetization with a high Curie temperature ( $T_C$ ) and a large coercive field ( $H_c$ ). This phenomenon is known to be caused by an optically charge-transfer-induced spin transition (CTIST) from  $\text{Co}^{\text{III}}_{\text{low-spin}(ls)}(S = 0) - \text{W}^{\text{IV}}(S = 0)$  to  $\text{Co}^{\text{II}}_{\text{high-spin}(hs)}(S = 3/2) - \text{W}^{\text{V}}(S = 1/2)$  phases. That is, light irradiation induces the charge transfer from  $\text{W}^{\text{IV}}(S = 0)$  to  $\text{Co}^{\text{III}}_{ls}(S = 0)$  to produce  $\text{Co}^{\text{II}}_{ls}(S = 1/2) - \text{W}^{\text{V}}(S = 1/2)$ , and then a spin transition occurs from  $\text{Co}^{\text{II}}_{ls}(S = 1/2)$  to  $\text{Co}^{\text{II}}_{hs}(S = 3/2)$ , which results in the electronic state of  $\text{Co}^{\text{II}}_{hs}(S = 3/2) - \text{W}^{\text{V}}(S = 1/2)$ . However, the electronic structure to discuss the optical transitions and the mechanism of photomagnetic effects has not been clarified yet. In the present work, a cobalt–octacyanidotungstate bimetal assembly,  $(\text{H}_5\text{O}_2^+)[\text{Co}^{\text{III}}(4\text{-bromopyridine})_2\{\text{W}^{\text{IV}}(\text{CN})_8\}]$  is reported. Interestingly, this compound exhibits the  $\text{Co}^{\text{III}}_{ls} - \text{W}^{\text{IV}}$  phase over a wide temperature range from 2 K to 390 K, even though all the other reported cobalt–octacyanidotungstate bimetal assemblies take the  $\text{Co}^{\text{II}}_{hs} - \text{W}^{\text{V}}$  phase at room temperature. A light irradiation to this compound causes photo-induced magnetization. First-principles calculations show the electronic structure of this compound to reveal the mechanism of the charge-transfer process.

## Results and Discussion

### Synthesis, crystal structure, and electronic state

The single crystal and the powder-form sample of  $(\text{H}_5\text{O}_2^+)[\text{Co}^{\text{III}}(4\text{-bromopyridine})_2\{\text{W}^{\text{IV}}(\text{CN})_8\}]$  were synthesized by mixing  $\text{Na}_3[\text{W}^{\text{V}}(\text{CN})_8]\cdot 4\text{H}_2\text{O}$ ,  $\text{Co}^{\text{II}}\text{Cl}_2\cdot 6\text{H}_2\text{O}$ , and 4-bromopyridine·HCl in an acidic condition at room temperature. Elemental analyses confirm that the formula of this compound is  $(\text{H}_5\text{O}_2)[\text{Co}(4\text{-bromopyridine})_2\{\text{W}(\text{CN})_8\}]$ .

Since the single crystals are in a very thin hexagonal plate-form (e.g., *ca.*  $100\times 50\times 4$   $\mu\text{m}$ ), a synchrotron radiation X-ray single-crystal measurement at KEK was carried out to determine the crystal structure. This compound has a monoclinic crystal structure in the  $P2_1/c$  space group ( $a = 13.0471(10)$   $\text{\AA}$ ,  $b = 13.5910(10)$   $\text{\AA}$ ,  $c = 14.6790(10)$   $\text{\AA}$ , and  $\beta = 106.3410(10)^\circ$ ). The asymmetric unit consists of a  $\text{Co}^{3+}$  ion, a  $[\text{W}(\text{CN})_8]^{4-}$  ion, two 4-bromopyridine ligands, and two water molecules. The coordination geometry of the Co site is a six-coordinate pseudo octahedron, in which the two axial positions of Co are occupied by the N atoms of 4-bromopyridine, and the four equatorial positions are occupied by the cyanide N atoms of  $[\text{W}(\text{CN})_8]^{4-}$ . The average distance of Co–N is 1.92  $\text{\AA}$ , indicating that the Co ion takes a trivalent state. The coordination geometry of the W site is an eight-coordinate square antiprism, where the four CN groups of  $[\text{W}(\text{CN})_8]^{4-}$  are bridged to Co. The other four CN groups are not bridged to Co, but connected to  $\text{H}_5\text{O}_2^+$  by hydrogen bonds. The cyanide-bridged Co and W ions form two-dimensional layers in the  $bc$ -plane, and the oxonium cations  $\text{H}_5\text{O}_2^+$  are intercalated between the layers. The  $\{\text{Co}^{\text{III}}[\text{W}^{\text{IV}}(\text{CN})_8]\}^-$  layers take negative charge, and the positive charge of  $\text{H}_5\text{O}_2^+$  keeps the whole charge of this compound neutral.

In the microscopic ultraviolet–visible measurement, the absorption peak for the

transmission mode along the direction of the out-of  $bc$ -plane is observed around 700 nm (1.8 eV). The magnetic susceptibility was measured by superconducting quantum interference device (SQUID) using the assembled single crystals (*c.a.*  $8 \times 10^5$  pieces of crystals). The  $\chi_M T$  value is almost zero from 2 K to 390 K, which indicates that this compound takes the electronic state of  $\text{Co}^{\text{III}}_{ls}(S=0)\text{-W}^{\text{IV}}(S=0)$  over the wide temperature range of 2–390 K. Such a stabilization of the  $\text{Co}^{\text{III}}_{ls}\text{-W}^{\text{IV}}$  phase over the wide temperature range has not been reported so far.

#### Periodic structure calculations

The periodic structure calculation of  $(\text{H}_5\text{O}_2^+)[\text{Co}^{\text{III}}(4\text{-bromopyridine})_2\{\text{W}^{\text{IV}}(\text{CN})_8\}]$  was performed by Vienna *ab initio* simulation package (VASP) to reveal the optical transitions of this compound, where the crystal structure determined by the single-crystal X-ray analysis was used. The band structure and the density of states (DOS) show that the band gap is composed of a W 5d valence band and a Co 3d conduction band. The calculated optical absorption spectrum reproduced well the experimental spectrum. The lowest-energy transition was a transition from the valence band mainly composed of  $d_{z^2}$  orbitals of W and p orbitals of N to the conduction band mainly contributed from  $d_{z^2}$  orbitals of Co and sp orbitals of N. This indicates that the lowest-energy transition of this compound is the charge transfer from  $\text{W}^{\text{IV}}$  to  $\text{Co}^{\text{III}}$  through the orbitals of the bridging CN ligands. Since the valence band from d orbitals of Co is below  $-3.5$  eV, the absorption of d-d transition in Co is not observed in the visible region. Thus, visible light irradiation does not caused the spin transition in  $\text{Co}^{\text{III}}$ .

#### Photo-induced phase transition

The photomagnetic effect was investigated using SQUID. The 785-nm light irradiation ( $220 \text{ mW cm}^{-2}$ ) at 3 K induced spontaneous magnetization. Magnetization ( $M$ ) versus temperature ( $T$ ) curve shows that a value of  $T_C$  is 27 K.  $M$  versus external magnetic field ( $H$ ) curve exhibits an  $H_c$  value of 2000 Oe at 2 K. Considering the ground Kramers doublet of an octahedral  $\text{Co}^{\text{II}}$ , an expected saturation magnetization ( $M_s$ ) value is  $3.2 \mu_B$  due to ferromagnetic coupling between  $\text{W}^{\text{V}}(S = 1/2, g = 2)$  and  $\text{Co}^{\text{II}}(S = 1/2, g = 13/3)$ , which is close to the observed  $M_s$  value of  $3.0 \mu_B$ . The photo-induced phase returns to the initial phase upon annealing up to 80 K. These light irradiation and heating treatment provide reversible phase changes.

To determine the crystal structure of photo-induced phase, the powder XRD pattern was measured after 785-nm light irradiation ( $250 \text{ mW cm}^{-2}$ ) at 13 K. Rietveld analysis of the XRD pattern after light irradiation shows that the photo-induced phase has a monoclinic structure in the  $P2_1/c$  space group with lattice constants of  $a = 13.193(10) \text{ \AA}$ ,  $b = 113.949(11) \text{ \AA}$ ,  $c = 15.040(12) \text{ \AA}$ , and  $\beta = 107.35(9)^\circ$ , which are larger in the two-dimensional layer ( $bc$ -plane) by 3% compared to the original phase. The average Co–N distance of photo-induced phase ( $2.05 \text{ \AA}$ ) is larger than that of original phase ( $1.91 \text{ \AA}$ ). Such an elongation indicates that the valence state of Co changes from +3 to +2 by light irradiation. After annealing up to 60 K, the crystal structure of photo-induced phase returned to that of the original phase.

The photo-induced magnetization can be explained by the optical CTIST effect from  $\text{Co}^{\text{III}}_{hs}(S = 0) - \text{W}^{\text{IV}}(S = 0)$  to  $\text{Co}^{\text{II}}_{hs}(S = 3/2) - \text{W}^{\text{V}}(S = 1/2)$  phases. When the temperature is under  $T_C$ , spontaneous magnetization is observed due to superexchange coupling between  $\text{Co}^{\text{II}}_{hs}(S = 3/2)$  and  $\text{W}^{\text{V}}(S = 1/2)$  through CN groups.

## Conclusions

In my thesis, a two-dimensional cyanide-bridged Co–W bimetal assembly,  $(\text{H}_5\text{O}_2^+)[\text{Co}^{\text{III}}(4\text{-bromopyridine})_2\{\text{W}^{\text{IV}}(\text{CN})_8\}]$  was synthesized. This compound shows a stable  $\text{Co}^{\text{III}}_{\text{ls}}\text{--W}^{\text{IV}}$  phase in the 2–390 K range. Such a wide temperature range  $\text{Co}^{\text{III}}_{\text{ls}}\text{--W}^{\text{IV}}$  phase has not been reported up to date. Light irradiation to this compound causes the photo-induced phase with a  $T_{\text{C}}$  value of 27 K and an  $H_{\text{c}}$  value of 2000 Oe. The crystal structures before and after light irradiation were determined by X-ray structural analyses. Additionally, first-principles calculations revealed that the photo-induced phase transition is due to the charge transfer from a W 5d valence band to a Co 3d conduction band.

# Contents

---

<b>Chapter 1 Introduction .....</b>	<b>4</b>
1.1. Background .....	4
1.1.1 Molecular based magnet.....	4
1.1.2 Magnetism.....	5
1.1.3 Cyanide-bridged metal assembly .....	9
1.1.4 Photo-induced phase transition .....	11
1.1.5 Photo-induced magnetization in cyanide-bridged metal assemblies based on octacyanidometalates .....	12
1.2. Objective and Outline .....	14
Figures and Tables.....	16
<b>Chapter 2 Synthesis, crystal structure, and characterization of a two-dimensional cobalt–octacyanidotungstate bimetal assembly.....</b>	<b>34</b>
2.1. Introduction.....	34
2.2. Experiments .....	35
2.2.1 Synthesis.....	35
2.2.2 Characterization .....	37
2.3. Results and Discussion.....	39
2.3.1 Elemental analyses .....	39
2.3.2 Crystal structure .....	39

2.3.3	Micro-IR and UV–vis spectroscopy.....	40
2.3.4	Magnetic property .....	41
2.3.5	TG measurement .....	41
2.3.6	Cyclic voltammetry .....	41
2.4.	Conclusions .....	42
	Figures and Tables.....	43

**Chapter 3 Periodic structure calculations of a two-dimensional cobalt–octacyanidotungstate bimetal assembly..... 61**

3.1.	Introduction.....	61
3.2.	Periodic structure calculations .....	62
3.3.	Results and discussion .....	62
3.3.1	Band structure, density of states, and calculated optical absorption spectrum.....	62
3.3.2	Charge density maps .....	63
3.4.	Conclusions .....	63
	Figures and Tables.....	65

**Chapter 4 Photo-induced magnetization of a two-dimensional cobalt–octacyanidotungstate bimetal assembly..... 70**

4.1.	Introduction.....	70
4.2.	Experiments .....	71
4.3.	Results and discussion .....	72



4.3.1	Magnetic measurements after light irradiation at low temperature.....	72
4.3.2	UV–vis measurements after light irradiation at low temperature .....	73
4.3.3	XRD measurements after light irradiation at low temperature .....	73
4.3.4	Mechanism .....	74
4.4.	Conclusions .....	75
	Figures and Tables.....	76
<b>Chapter 5</b>	<b>Summary and perspective.....</b>	<b>89</b>
<b>References</b>	<b>.....</b>	<b>92</b>
<b>List of paper related to the thesis</b>	<b>.....</b>	<b>101</b>
<b>Acknowledgements</b>	<b>.....</b>	<b>102</b>

# Chapter 1

## Introduction

---

### 1.1. Background

#### 1.1.1 Molecular based magnet

Magnetic materials have been used for various applications such as magnetic recording media,<sup>1</sup> permanent magnets,<sup>2</sup> and electromagnetic wave absorbers.<sup>3</sup> Conventional magnets were inorganic materials, for example, metals, metal alloys, and metal oxides. However, some types of metal complexes were reported to exhibit ferromagnetism,<sup>4</sup> revealing that molecular based materials are good candidates for magnetic materials. In molecular based magnets, metal ions of metal complexes or/and organic radicals are used as spin origin. As crystal structures and electronic states of molecular based magnets change by external stimuli, their magnetism can be controlled by external stimuli. Molecular based magnets have high designability because selection of metal ions and organic ligands of molecular based magnets controls the crystal structures, the magnetic properties, and other physical properties and functionalities. In the case of the molecular based magnets, various functionalities which have not been achieved in conventional magnets are expected. Photo-induced magnetization,<sup>5-12</sup> humidity and alcohol vapor responsivity,<sup>13,14</sup> chirality,<sup>15</sup> ferroelectricity,<sup>16</sup> ion conductivity,<sup>17</sup> and magnetization-induced second harmonic generation (MSHG)<sup>18</sup> have been reported.

### 1.1.2 Magnetism

#### Paramagnetism<sup>19</sup>

When magnetic moments  $M$  exist in an external field  $H$ , potential energy  $E(\theta)$  is expressed as

$$E(\theta) = -MH \cos \theta,$$

where  $\theta$  is the angle between  $M$  and  $H$ . A direction along  $H$  is  $z$ -axis. Given Boltzmann distribution, probability that  $M$  faces the direction of  $\theta$  from  $z$ -axis is proportional to

$$\exp\left(-\frac{E(\theta)}{k_B T}\right) = \exp\left(\frac{MH \cos \theta}{k_B T}\right), \quad (\text{Equation 1.1})$$

where  $k_B$  is Boltzmann constant and  $T$  is temperature. Probability that  $M$  is oriented in the direction between  $\theta$  and  $\theta + d\theta$  is represented as

$$p(\theta)d\theta = \frac{\exp\left(\frac{MH \cos \theta}{k_B T}\right) \cdot 2\pi \sin \theta d\theta}{\int_0^\pi \exp\left(\frac{MH \cos \theta}{k_B T}\right) \cdot 2\pi \sin \theta d\theta} = \frac{\exp\left(\frac{MH \cos \theta}{k_B T}\right) \sin \theta d\theta}{\int_0^\pi \exp\left(\frac{MH \cos \theta}{k_B T}\right) \sin \theta d\theta}. \quad (\text{Equation 1.2})$$

Magnetization  $I$  are expressed as  $z$  component of  $M$ , and the average of  $I$  is taken by  $\theta$  to be represented as

$$\begin{aligned} I &= NM \overline{\cos \theta} = NM \int_0^\pi \cos \theta p(\theta) d\theta = NM \frac{\int_0^\pi \exp\left(\frac{MH \cos \theta}{k_B T}\right) \sin \theta \cos \theta d\theta}{\int_0^\pi \exp\left(\frac{MH \cos \theta}{k_B T}\right) \sin \theta d\theta} \\ &= NM \frac{\int_{-1}^1 x e^{\alpha x} dx}{\int_{-1}^1 e^{\alpha x} dx} \quad \left( \frac{MH}{k_B T} = \alpha, \cos \theta = x \right) \\ &= NM \left( \coth \alpha - \frac{1}{\alpha} \right) = NML(\alpha), \end{aligned} \quad (\text{Equation 1.3})$$

where  $N$  is the number of  $M$ , and  $L(\alpha)$  is Langevin function. When  $\alpha \ll 1$ ,

$$I = NM \frac{\alpha}{3} = \frac{NM^2}{3k_B T} H. \quad (\text{Equation 1.4})$$

In the above, it is assumed that each magnetic moment is able to face every direction. However, it can be oriented only in the restricted direction because of quantization.  $z$  component of the magnetic moment  $M_z$  is expressed as

$$M_z = g\mu_B J_z, \quad (\text{Equation 1.5})$$

where  $g$  is Landé  $g$ -factor,  $\mu_B$  is Bohr magneton, and  $J_z$  is  $z$  component of the total angular momentum.

$J_z$  can take  $2J + 1$  values,

$$J_z = J, J-1, \dots, -(J-1), -J,$$

where  $J$  is total angular momentum quantum number. The average of  $I$  is taken by  $\theta$  to be represented as

$$\begin{aligned} I &= Ng\mu_B \frac{\sum_{J_z=-J}^J J_z \exp\left(\frac{g\mu_B H}{k_B T} J_z\right)}{\sum_{J_z=-J}^J \exp\left(\frac{g\mu_B H}{k_B T} J_z\right)} \\ &= Ng\mu_B J \left( \frac{2J+1}{2J} \coth \frac{2J+1}{2J} \alpha - \frac{1}{2J} \coth \frac{\alpha}{2J} \right) \quad \left( \alpha = \frac{g\mu_B H}{k_B T} J \right) \\ &= Ng\mu_B J B_J(\alpha), \end{aligned} \quad (\text{Equation 1.6})$$

where  $B_J(\alpha)$  is Brillouin function. When  $\alpha \ll 1$ ,

$$I = Ng\mu_B J \frac{J+1}{3J} \alpha = \frac{(g\mu_B)^2}{3k_B T} J(J+1)H. \quad (\text{Equation 1.7})$$

Therefore, magnetic susceptibility  $\chi = \frac{\partial I}{\partial H}$  is represented as

$$\chi = \frac{N(g\mu_B)^2}{3k_B T} J(J+1). \quad (\text{Equation 1.8})$$

As the orbital angular momentum disappears due to ligand field in a transition metal ion,  $J$  can be replaced by spin angular momentum quantum number  $S$  and expressed as

$$\chi = \frac{N(g\mu_B)^2}{3k_B T} S(S+1). \quad (\text{Equation 1.9})$$

Such a law that magnetic susceptibility is proportional to  $T^{-1}$  is called Curie's law. The product of molar magnetic susceptibility  $\chi_M$  and  $T$  is represented as

$$\chi_M T = \frac{(g\mu_B)^2}{3k_B} S(S+1) \approx \frac{1}{8} g^2 S(S+1). \quad (\text{Equation 1.10})$$

When several metal ions exist,

$$\chi_M T = \sum_i \frac{1}{8} g_i^2 S_i(S_i+1), \quad (\text{Equation 1.11})$$

which is called spin-only value. By comparing the expected value from this equation and the observed value,  $S_i$  values can be estimated.

### Ferromagnetism<sup>19</sup>

When molecular magnetic field  $H_m$  generated by surrounding spins acts on each spin,  $H_m$  is expressed as

$$H_m = nI \quad \left( n = \frac{Z}{N(g\mu_B)^2} J \right), \quad (\text{Equation 1.12})$$

where  $I$  is magnetization,  $Z$  is number of neighbor sites, and  $J$  is superexchange interaction constant between spins. When external magnetic field  $H_{ex}$  acts on the system, total magnetic fields acting on each spin,  $H$ , is represented as

$$H = H_{ex} + H_m = H_{ex} + nI. \quad (\text{Equation 1.13})$$

The explanation about paramagnetism is also applied in this case.  $I$  is expressed as

$$I = Ng\mu_B SB_S(\alpha) = Ng\mu_B S \left( \frac{2S+1}{2S} \coth \frac{2S+1}{2S} \alpha - \frac{1}{2S} \coth \frac{\alpha}{2S} \right), \quad (\text{Equation 1.14})$$

$$\text{where } \alpha = \frac{g\mu_B H}{k_B T} S = \frac{g\mu_B S(H_{\text{ex}} + nI)}{k_B T}.$$

$$\therefore I = \frac{k_B T}{g\mu_B Sn} \alpha - \frac{H_{\text{ex}}}{n}. \quad (\text{Equation 1.15})$$

The solutions of  $I$  and  $\alpha$  which satisfy two above equations at the same time should be found. That is, when the equations are regarded as functions depend on  $\alpha$ , the intersection of the functions is obtained. Below a Curie temperature ( $T_C$ ), spontaneous magnetization is generated at  $H_{\text{ex}} = 0$ . As  $I$  becomes a plus value just at  $T_C$ , the differentials of the functions at  $\alpha = 0$  take the same value at  $T_C$  (Figure 1.1). That is,

$$\left( \frac{\partial I}{\partial \alpha} \right)_{\alpha=0} = Ng\mu_B S \frac{S+1}{3S} = \frac{k_B T_C}{g\mu_B Sn}. \quad (\text{Equation 1.16})$$

$$\therefore T_C = \frac{N(g\mu_B)^2 S(S+1)n}{3k_B} = \frac{ZJS(S+1)}{3k_B}. \quad (\text{Equation 1.17})$$

Additionally, this equation is expanded to multi-component system. Total magnetic field acting on  $i$  site ( $H_i$ ) is expressed as

$$H_i = H_{\text{ex}} + \sum_j n_{ij} I_j \quad \left( n_{ij} = \frac{Z_{ij}}{N_j (g_j \mu_B)^2} J_{ij} \right). \quad (\text{Equation 1.18})$$

Similarly in the case of unitary system,  $I$  is expressed as

$$I_i = N_i g_i \mu_B S_i B_S(\alpha_i), \quad (\text{Equation 1.19})$$

$$\text{where } \alpha_i = \frac{g_i \mu_B H_i}{k_B T} S_i = \frac{g_i \mu_B S_i \left( H_{\text{ex}} + \sum_j n_{ij} I_j \right)}{k_B T}.$$

When  $H_{\text{ex}} = 0$  and  $T = T_C$ , by the approximation  $B_S(\alpha_i) \approx \frac{S_i+1}{3S_i} \alpha_i$ ,  $I$  is represented as

$$I_i = N_i g_i \mu_B S_i \frac{S_i + 1}{3S_i} \alpha_i = N_i g_i \mu_B S_i \frac{S_i + 1}{3S_i} \frac{g_i \mu_B S_i \sum_j n_{ij} I_j}{k_B T_C} = \frac{N_i (g_i \mu_B)^2 S_i (S_i + 1)}{3k_B T_C} \sum_j n_{ij} I_j .$$

(Equation 1.20)

For example, in the case of binary system,

$$\begin{cases} I_A = \frac{N_A (g_A \mu_B)^2 S_A (S_A + 1)}{3k_B T_C} n_{AB} I_B \\ I_B = \frac{N_B (g_B \mu_B)^2 S_B (S_B + 1)}{3k_B T_C} n_{BA} I_A \end{cases} .$$

(Equation 1.21)

$$\begin{aligned} \therefore I_A &= \frac{N_A (g_A \mu_B)^2 S_A (S_A + 1)}{3k_B T_C} n_{AB} \frac{N_B (g_B \mu_B)^2 S_B (S_B + 1)}{3k_B T_C} n_{BA} I_A \\ &= \frac{n_{AB} n_{BA} N_A N_B (g_A \mu_B)^2 (g_B \mu_B)^2 S_A (S_A + 1) S_B (S_B + 1)}{(3k_B T_C)^2} I_A \\ &= \frac{J_{AB}^2 Z_{AB} Z_{BA} S_A (S_A + 1) S_B (S_B + 1)}{(3k_B T_C)^2} I_A . \end{aligned}$$

(Equation 1.22)

$$\therefore T_C = \frac{|J_{AB}|}{3k_B} \sqrt{Z_{AB} Z_{BA} S_A (S_A + 1) S_B (S_B + 1)} .$$

(Equation 1.23)

Using this equation, superexchange interaction ( $J_{AB}$ ) between metal ions can be estimated from the observed  $T_C$  value.

### 1.1.3 Cyanide-bridged metal assembly

A cyanide-bridged metal assembly is a system composed of metal ions bridged by cyanide groups. Building blocks such as hexacyanidometalate [ $M(\text{CN})_6$ ], heptacyanidometalate [ $M(\text{CN})_7$ ], and octacyanidometalate [ $M(\text{CN})_8$ ], are used to synthesize cyanide-bridged metal assemblies (Figure 1.2). Cyanide-bridged metal assemblies with various crystal structures can be synthesized by combination of building

blocks, metal ions, and organic ligands.<sup>20</sup>

### Cyanide-bridged metal assembly based on hexacyanidometalate

Prussian blue,  $\text{Fe}^{\text{III}}_4[\text{Fe}^{\text{II}}(\text{CN})_6]_3 \cdot 4\text{H}_2\text{O}$ , is the most famous cyanide-bridged metal assembly and consists of hexacyanidometalate. Metal ions in Prussian blue can be substituted by the other metal ions, and alkali cations can be implemented in the crystal structure. Such a system is known as Prussian blue analog (PBA) (Figure 1.3). PBA has received attention in a study field of molecular magnets because PBA has a three-dimensional network structure and can form a magnetic interactive network with three-dimensional expanse, expecting that PBA can exhibit a high Curie temperature ( $T_C$ ). A vanadium–hexacyanidochromate Prussian blue analog,  $\text{V}^{\text{II}}_{0.42}\text{V}^{\text{III}}_{0.58}[\text{Cr}(\text{CN})_6]_{0.86} \cdot 2.8\text{H}_2\text{O}$ , was reported to show a Curie temperature above room temperature ( $T_C = 315 \text{ K}$ ).<sup>21</sup> PBA has also been reported to exhibit various functionalities. PBA containing Co and Fe,  $\text{K}_{0.2}\text{Co}_{0.4}[\text{Fe}(\text{CN})_6]$ , was reported to exhibit photo-induced magnetization for the first time.<sup>5a</sup> Our laboratory has reported mixed ferro-ferri magnetism,<sup>22</sup> two compensation temperature,<sup>23</sup> photo-induced magnetic pole inversion,<sup>6</sup> humidity sensitive magnetism,<sup>13</sup> spin ionics,<sup>17a</sup> zero thermal expansion,<sup>24</sup> ferromagnetic and ferroelectric coexistence,<sup>16</sup> and ammonium adsorption.<sup>25</sup>

### Cyanide-bridged metal assembly based on octacyanidometalate

A coordination environment in hexacyanidometalate is six-coordinate octahedron, whereas octacyanidometalate can take various coordination environments such as square antiprism, dodecahedron, and bicapped trigonal prism dependently on surrounding environment (Figure 1.4).<sup>26</sup> Due to such variety of coordination environments, cyanide-



bridged metal assemblies based on octacyanidometalates take various crystal structures. Additionally, octacyanidometalates have high coordination number, and their diffuse 4d or 5d orbitals of the center metal ion enhance superexchange interaction. Therefore, octacyanidometalates are useful building blocks to form molecular based magnets. By incorporating organic ligands, cyanide-bridged metal assemblies based on octacyanidometalates take various dimensional crystal structure such as zero-dimensional cluster structures (Figure 1.5),<sup>27</sup> one-dimensional chain structures (Figure 1.6),<sup>28</sup> two-dimensional layer structures (Figure 1.7),<sup>29</sup> and three-dimensional network structures (Figure 1.8).<sup>30</sup> Since center metal ions in octacyanidometalates take various electronic states, for example,  $\text{Mo}^{\text{IV/V}}$  and  $\text{W}^{\text{IV/V}}$ , cyanide-bridged metal assemblies composed of the octacyanidometalates and appropriate metal ions are expected to exhibit charge-transfer phase transition by external stimuli such as temperature, photo, and pressure. The charge-transfer phase transition affects the magnetic properties of cyanide-bridged metal assemblies because the magnetic properties are dependent on the electronic states of the metal ions. Our laboratory has reported photo-induced magnetization caused by the charge transfer.<sup>10,11</sup> We have also presented magnetic materials based on octacyanidometalates with various functionalities, for example, high Curie temperature,<sup>31</sup> high thermal durability,<sup>32</sup> luminescence,<sup>33</sup> spin crossover photomagnetism,<sup>12</sup> and 90-degree optical-switching of output second harmonic light.<sup>12b</sup>

#### 1.1.4 Photo-induced phase transition

Photo-induced phase transition has received extensive attention as one of the attractive issues of non-equilibrium phenomena.<sup>34</sup> Additionally, photo-induced phase

transition materials are expected to be used for applications such as optical memory device and optical sensor.<sup>35</sup> Several types of them have been reported so far, for example, chalcogenides,<sup>36</sup> metal oxides,<sup>37</sup> spin-crossover complexes,<sup>38</sup> and cyanide-bridged bimetal assemblies.<sup>39</sup> Our laboratory has reported a titanium oxide exhibiting photo-reversible phase transition at room<sup>37b</sup> and cyanide-bridged metal assemblies showing photomagnetism based on photo-induced phase transition.<sup>6,7,9-12</sup>

#### 1.1.5 Photo-induced magnetization in cyanide-bridged metal assemblies based on octacyanidometalates

Our laboratory has studied three types of photomagnets based on octacyanidometalates, containing Cu–Mo,<sup>10</sup> Co–W,<sup>11</sup> and Fe–Nb.<sup>12</sup> Before light irradiation, all of the systems show paramagnetism. Light irradiation produces spontaneous magnetization. The magnetization disappears by annealing or/and light irradiation. The mechanism of photomagnetism in these systems are different, and details are described below.

##### Copper–octacyanidomolybdate bimetal assembly

Photomagnets containing Cu–Mo have two-dimensional layer or three-dimensional network structures (Figure 1.9).<sup>10</sup> The mechanism of the photomagnets is photo-induced charge transfer. Before irradiation, these compounds take  $\text{Cu}^{\text{II}}(S = 1/2)\text{--Mo}^{\text{IV}}(S = 0)$  state, and light irradiation induces charge transfer to produce  $\text{Cu}^{\text{I}}(S = 0)\text{--Mo}^{\text{V}}(S = 1/2)$ . Since stoichiometric ratio of the metal ions are Cu : Mo = 2 : 1,  $\text{Cu}^{\text{II}}(S = 1/2)$  remains in the system. Spontaneous magnetization is observed below  $T_c$  by ferromagnetic interaction

between the  $\text{Mo}^{\text{V}}(S = 1/2)$  ions produced by light irradiation and the remained  $\text{Cu}^{\text{II}}(S = 1/2)$  ions. However, the different mechanism, where light irradiation induces spin crossover from  $\text{Mo}^{\text{IV}}(S = 0)$  to  $\text{Mo}^{\text{IV}}(S = 1)$ , have been proposed. Recently, periodic structure calculations have revealed optical transitions of  $\text{Cu}_2[\text{Mo}(\text{CN})_8] \cdot 8\text{H}_2\text{O}$ , showing charge transfer is induced by visible light irradiation in this compound.<sup>10d</sup>

### Iron–octacyanidonioabate bimetal assembly

Iron–octacyanidonioabate photomagnets have three-dimensional network structure (Figure 1.10).<sup>12</sup> The photomagnetism mechanism in this system is light-induced excited spin state trapping (LIESST). These compound shows  $\text{Fe}^{\text{II}}_{\text{hs}}(S = 0)–\text{Nb}^{\text{IV}}(S = 1/2)$  state, and light irradiation induces spin crossover to produce the electronic state of  $\text{Fe}^{\text{II}}_{\text{hs}}(S = 2)–\text{Nb}^{\text{IV}}(S = 1/2)$ , showing photo-induced magnetization. Our laboratory reported  $\text{Fe}_2[\text{Nb}(\text{CN})_8](4\text{-pyridinealdoxime})_8 \cdot 2\text{H}_2\text{O}$ , which is the first example of a spin crossover photomagnet.<sup>12a</sup> A chiral photomagnet  $\text{Fe}_2[\text{Nb}(\text{CN})_8](4\text{-bromopyridine})_8 \cdot 2\text{H}_2\text{O}$ , exhibiting 90-degree optical-switching of output second harmonic light,<sup>12b</sup> and a spin crossover photomagnet  $\text{Fe}_2[\text{Nb}(\text{CN})_8](4\text{-methylpyridine})_8 \cdot 2\text{H}_2\text{O}$ , showing two-step spin crossover,<sup>12d</sup> were also reported.

### Cobalt–octacyanidotungstate bimetal assembly

Our laboratory has reported three cobalt–octacyanidotungstate bimetal assemblies exhibiting charge-transfer phase transition with large thermal hysteresis,  $\text{CsCo}[\text{W}(\text{CN})_8](3\text{-cyanopyridine})_2 \cdot \text{H}_2\text{O}$  (Figures 1.11 and 1.12),<sup>11a,11b</sup>  $\text{Co}_3[\text{W}(\text{CN})_8]_2(\text{pyrimidine})_4 \cdot 6\text{H}_2\text{O}$  (Figures 1.13, 1.14, and 1.15),<sup>11c,d,f</sup> and  $\text{Co}[\text{W}(\text{CN})_8]_2(\text{pyrimidine})_2(4\text{-methylpyridine})_2 \cdot 6\text{H}_2\text{O}$  (Figures 1.15 and 1.16).<sup>11e</sup> The

charge-transfer phase transition is a phase transition between  $\text{Co}^{\text{II}}_{hs}\text{-W}^{\text{V}}$  and  $\text{Co}^{\text{III}}_{ls}\text{-W}^{\text{IV}}$  phases. All of the cobalt–octacyanidotungstate bimetal assemblies show the  $\text{Co}^{\text{II}}_{hs}\text{-W}^{\text{V}}$  phase at room temperature and the  $\text{Co}^{\text{III}}_{ls}\text{-W}^{\text{IV}}$  phase at low temperature. The phase transition is known as charge-transfer-induced spin transition (CTIST) because spin transition in Co ion occurs accompanied by charge transfer between Co and W ions (Figure 1.17). Additionally, these cobalt–octacyanidotungstate bimetal assemblies exhibit photo-induced magnetization at low temperature. The mechanism of photomagnetism is thought to be optical CTIST. That is, light irradiation induces charge transfer from  $\text{W}^{\text{IV}}(S = 0)$  to  $\text{Co}^{\text{III}}_{ls}(S = 0)$  generating  $\text{Co}^{\text{II}}_{ls}(S = 1/2)\text{-W}^{\text{V}}(S = 1/2)$ , and then spin transition in Co ion occurs, producing the  $\text{Co}^{\text{II}}_{hs}(S = 3/2)\text{-W}^{\text{V}}(S = 1/2)$  phase. Ferromagnetism is observed below a Curie temperature due to superexchange interaction between  $\text{Co}^{\text{II}}_{hs}(S = 3/2)$  and  $\text{W}^{\text{V}}(S = 1/2)$  ions (Figure 1.18). These cobalt–octacyanidotungstate photomagnets have high Curie temperatures and large coercive fields. For example,  $\text{Co}[\text{W}(\text{CN})_8]_2(\text{pyrimidine})_2(4\text{-methylpyridine})_2 \cdot 6\text{H}_2\text{O}$  exhibits photo-induced magnetization with the highest Curie temperature and the largest coercive field in photomagnets.<sup>12b</sup> Moreover, our laboratory has also reported cobalt–octacyanidotungstate bimetal assemblies with various functionalities such as chiral magnets,<sup>15</sup> high thermal durability,<sup>32b,c</sup> and single molecule magnetic (SMM) and single chain magnetic (SCM) behaviors.<sup>40</sup>

## 1.2. Objective and Outline

In my thesis, I have focused on cobalt–octacyanidotungstate bimetal assemblies because they are photomagnets exhibiting high Curie temperature and large coercive field.

The photo-induced magnetization is thought to be caused by an optical charge-transfer-induced spin transition. However, theoretical calculations have not been conducted in cobalt–octacyanidotungstate bimetal assemblies and the mechanism of photomagnetism has not been clarified yet. From such a background, the objective in my thesis is the investigation of the photo-induced magnetization mechanism in cobalt–octacyanidotungstate bimetal assemblies.

In Chapter 2, the synthetic method, the crystal structure, and the magnetic properties of  $(\text{H}_5\text{O}_2^+)[\text{Co}^{\text{III}}(4\text{-bromopyridine})_2\{\text{W}^{\text{IV}}(\text{CN})_8\}]$  are examined. A synchrotron radiation X-ray single-crystal measurement at KEK reveals the crystal structure. Magnetic measurements elucidate that the electronic state of this compound takes  $\text{Co}^{\text{III}}(S = 0)\text{--}\text{W}^{\text{IV}}(S = 0)$  between 2 K and 390 K.

In Chapter 3, periodic structure calculations using the crystal structure of  $(\text{H}_5\text{O}_2^+)[\text{Co}^{\text{III}}(4\text{-bromopyridine})_2\{\text{W}^{\text{IV}}(\text{CN})_8\}]$  are presented, and optical transitions are discussed, revealing the mechanism of the charge-transfer process.

In Chapter 4, photomagnetic effect of  $(\text{H}_5\text{O}_2^+)[\text{Co}^{\text{III}}(4\text{-bromopyridine})_2\{\text{W}^{\text{IV}}(\text{CN})_8\}]$  is studied. Additionally, the crystal structure of photo-induced phase is determined by powder X-ray diffraction measurement.

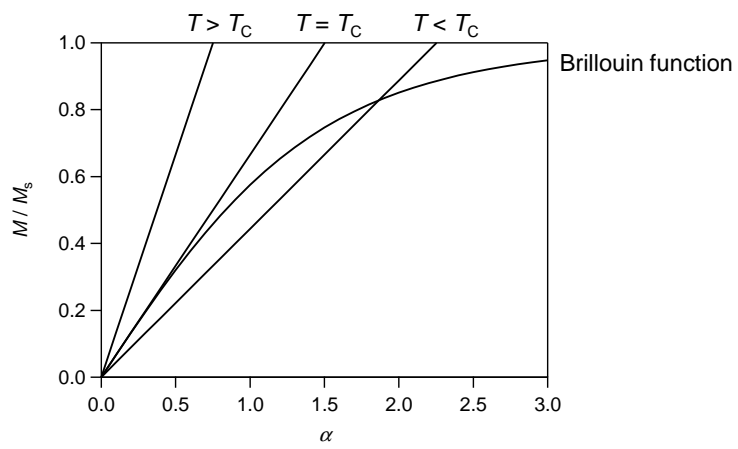


**Figure 1.1** Brillouin function and straight lines at  $T > T_c$ ,  $T = T_c$ , and  $T < T_c$ .

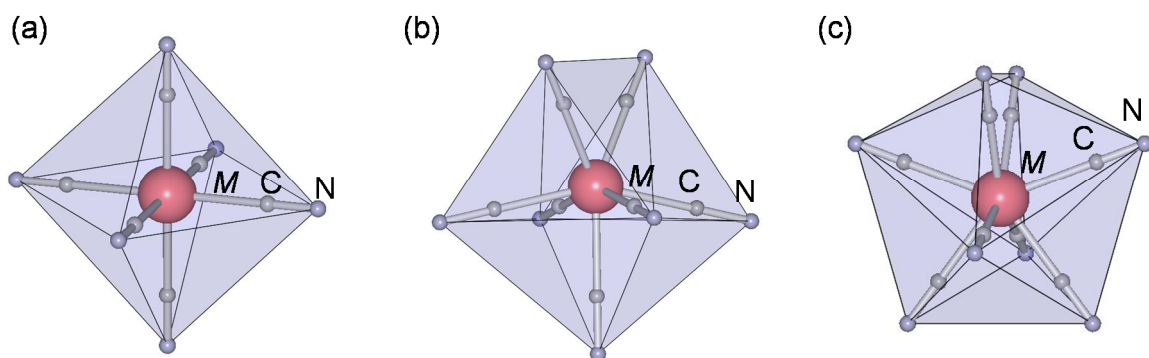


**Figure 1.2** Typical coordination environments of (a) hexacyanidometalate  $[M(CN)_6]^{n-}$ , (b) heptacyanidometalate  $[M(CN)_7]^{n-}$ , and (c) octacyanidometalate  $[M(CN)_8]^{n-}$ .

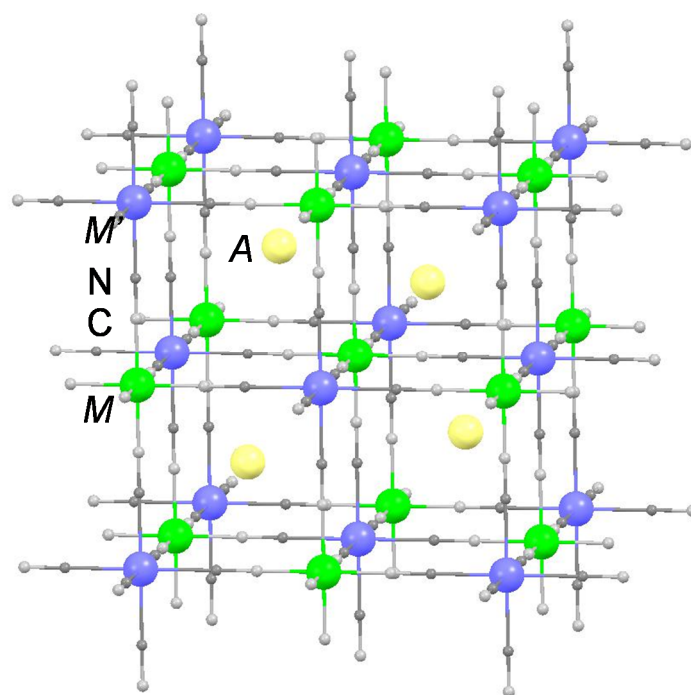


**Figure 1.3** Crystal structure of Prussian blue analog  $AM'[M(CN)_6]$ .



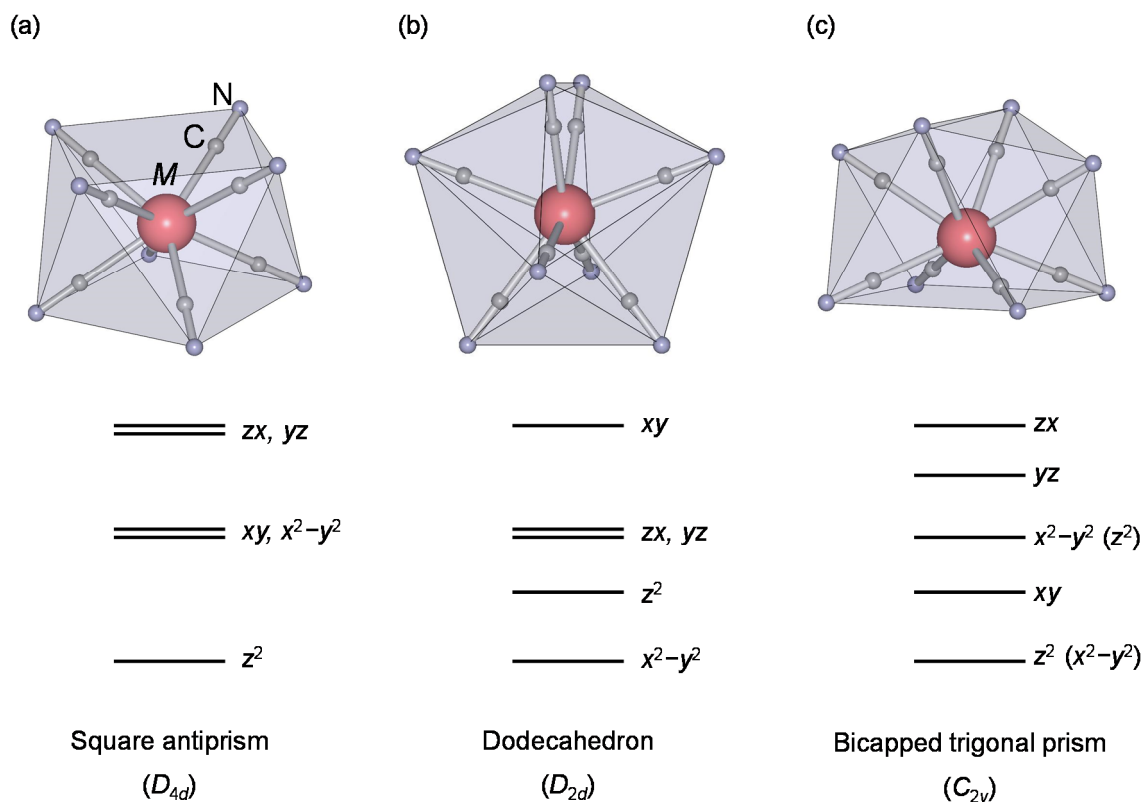


**Figure 1.4** Typical coordination environments of octacyanidometalate  $[M(CN)_8]^{n-}$  and energy diagrams of d orbitals. Reprinted with permission from ref. 26b. Copyright 2005 Elsevier B.V.

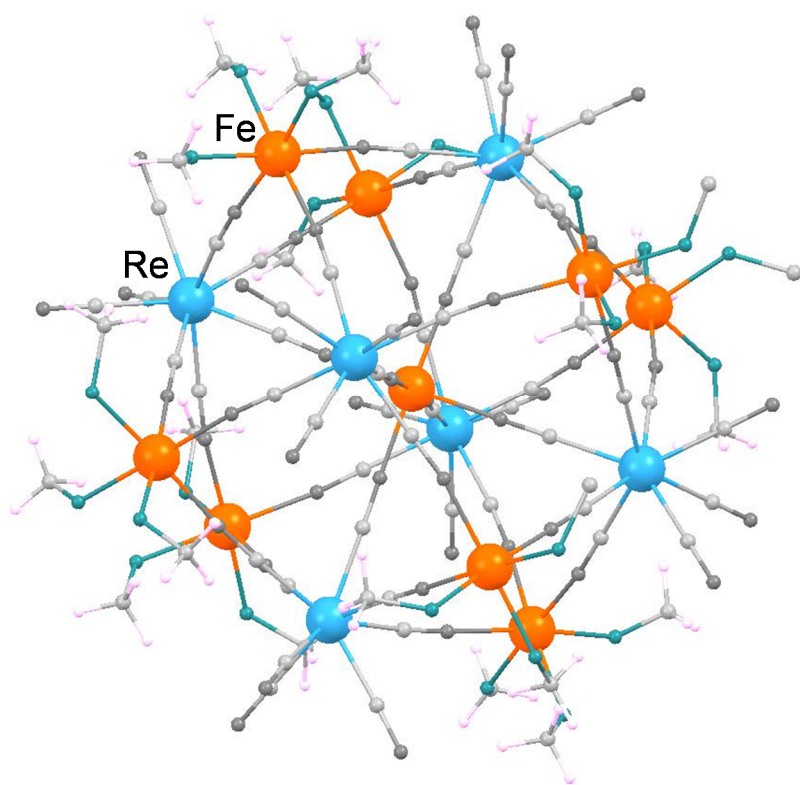


**Figure 1.5** Crystal structure of  $\{\text{Fe}^{\text{II}}_9[\text{Re}^{\text{V}}(\text{CN})_8]_6(\text{MeOH})_{24}\} \cdot 10\text{MeOH}$  (zero-dimensional compound). Reprinted with permission from ref. 27h. Copyright 2015 WILEY-VCH Verlag GmbH & Co. KGaA, Weinheim.

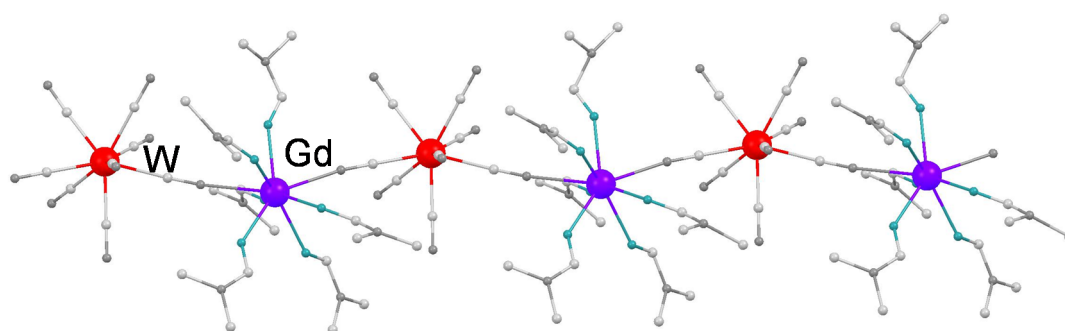


**Figure 1.6** Crystal structure of  $\text{Gd}^{\text{III}}(\text{dimethylformamide})_6[\text{W}^{\text{V}}(\text{CN})_8]$  (one-dimensional compound). Reprinted with permission from ref. 28d. Copyright 2005 Royal Society of Chemistry.

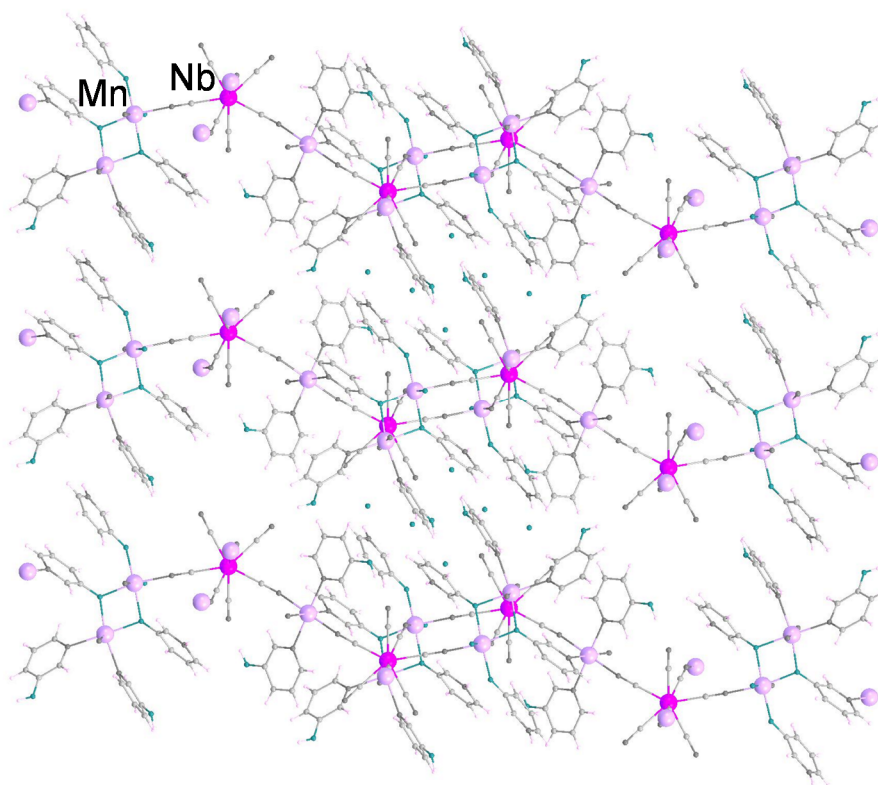


**Figure 1.7** Crystal structure of  $[\text{Mn}_5\{\text{Nb}(\text{CN})_8\}_2(3\text{-hydroxypyridine})_{12}]\cdot 6\text{H}_2\text{O}$  (two-dimensional compound). Reprinted with permission from ref. 29e. Copyright 2012 Elsevier B.V.

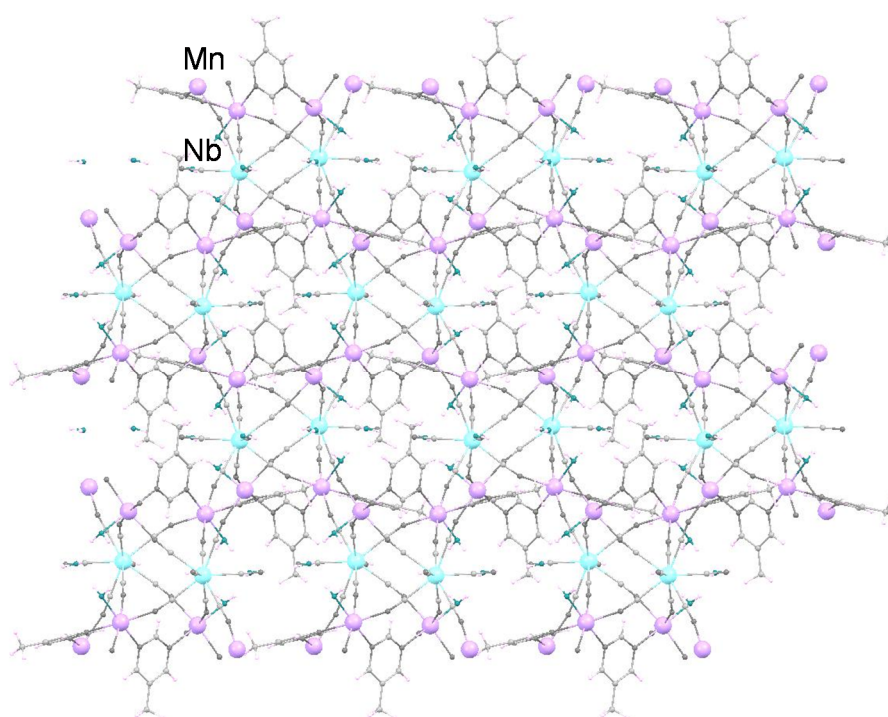


**Figure 1.8** Crystal structure of  $\text{Mn}_2[\text{Nb}(\text{CN})_8](5\text{-methylpyrimidine})_2 \cdot 4\text{H}_2\text{O}$  (three-dimensional compound). Reprinted with permission from ref. 30f. Copyright 2014 Elsevier B.V.

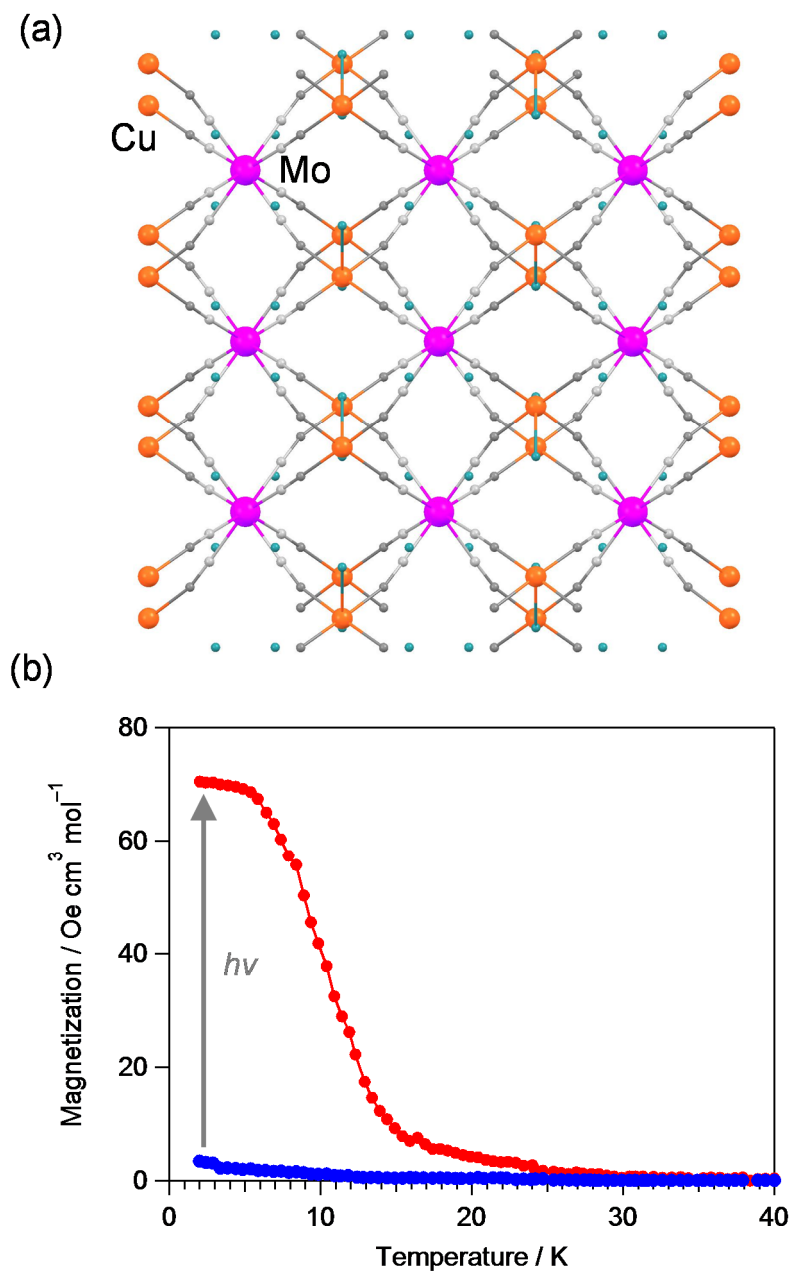


**Figure 1.9** (a) Crystal structure of  $\text{Cu}_2[\text{Mo}(\text{CN})_8] \cdot 8\text{H}_2\text{O}$ . Reprinted with permission from 10d. 30f. Copyright 2016 WILEY-VCH Verlag GmbH & Co. KGaA, Weinheim. (b) Photo-induced magnetization of  $\text{Cu}_2[\text{Mo}(\text{CN})_8] \cdot 8\text{H}_2\text{O}$ . Reprinted with permission from ref. 10b. Copyright 2006 American Chemical Society.

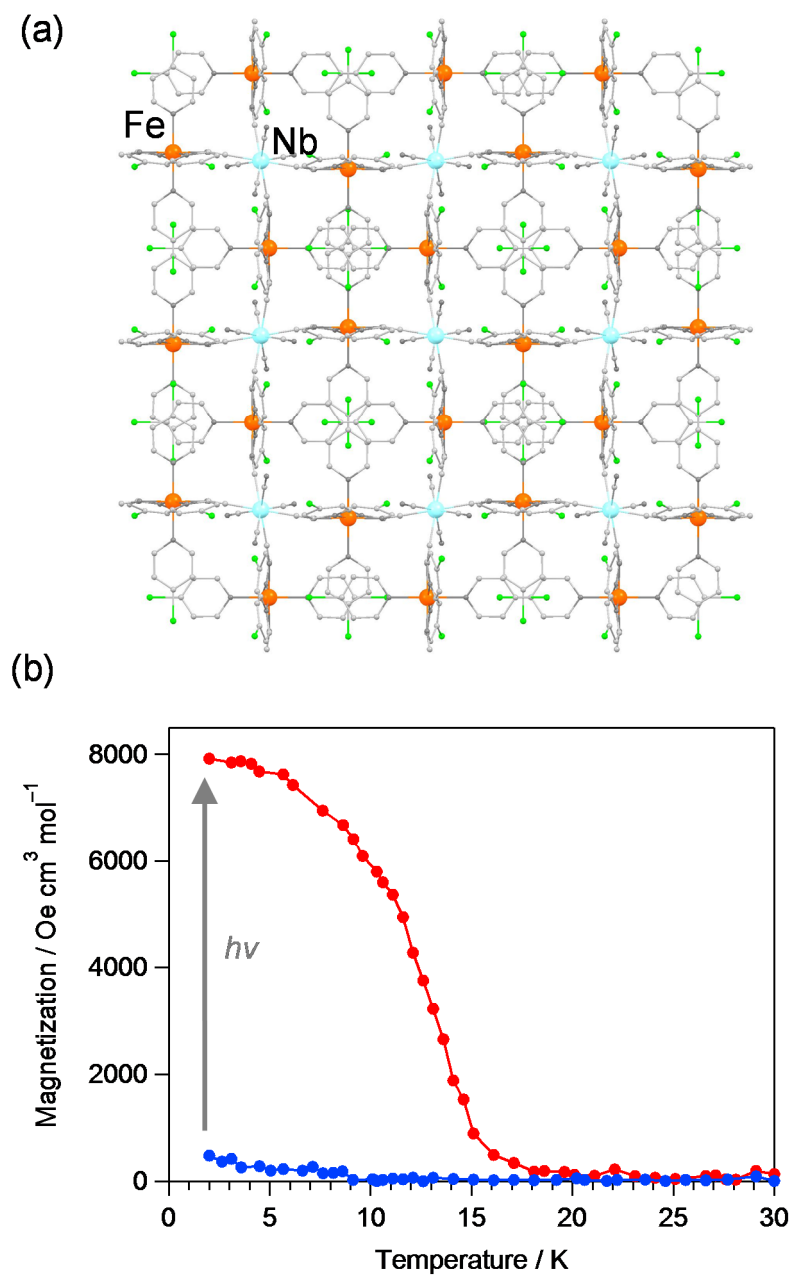


**Figure 1.10** (a) Crystal structure and (b) photo-induced magnetization of  $\text{Fe}_2[\text{Nb}(\text{CN})_8](4\text{-bromopyridine})_8 \cdot 2\text{H}_2\text{O}$ . Reprinted with permission from ref. 12b. Copyright 2013 Nature Publishing Group.

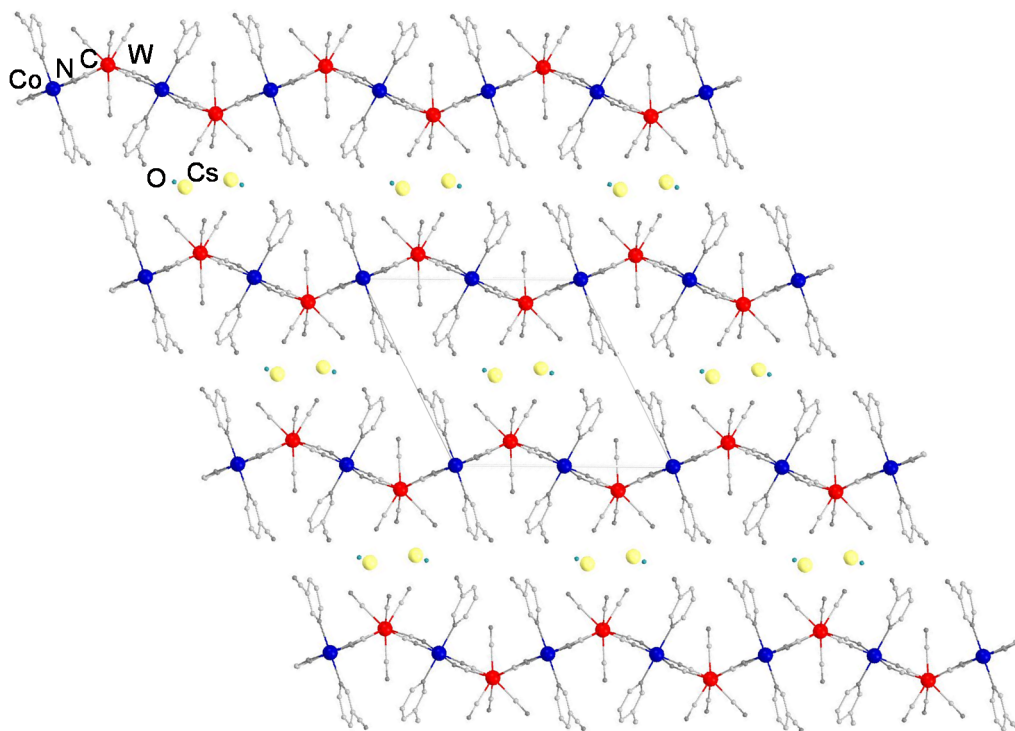


**Figure 1.11** Crystal structure of Cs[Co(3-cyanopyridine)<sub>2</sub>{W(CN)<sub>8</sub>}]·H<sub>2</sub>O. Reprinted with permission from ref. 11a. Copyright 2003 American Chemical Society.



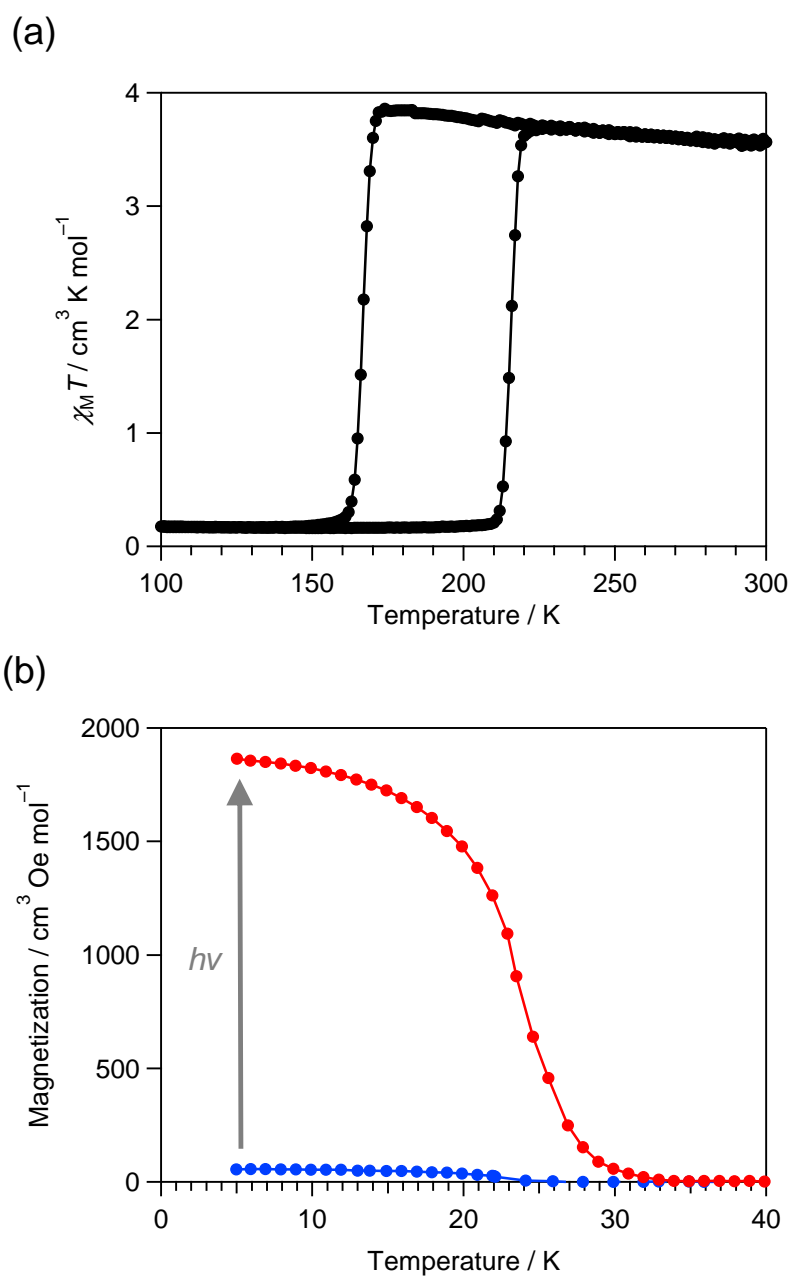


**Figure 1.12** (a) Thermal phase transition and (b) photomagnetic phenomenon of  $\text{Cs}[\text{Co}(\text{3-cyanopyridine})_2\{\text{W}(\text{CN})_8\}]\cdot\text{H}_2\text{O}$ . Reprinted with permission from ref. 11a. Copyright 2003 American Chemical Society.

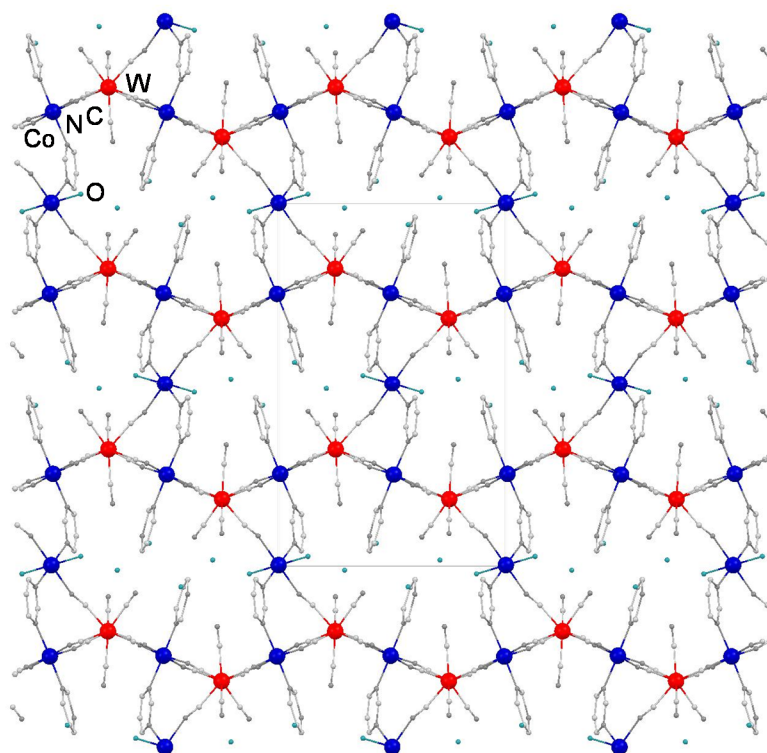


**Figure 1.13** Crystal structure of  $\text{Co}_3[\text{W}(\text{CN})_8]_2(\text{pyrimidine})_4 \cdot 6\text{H}_2\text{O}$ . Reprinted with permission from ref. 11c. Copyright 2008 American Chemical Society.

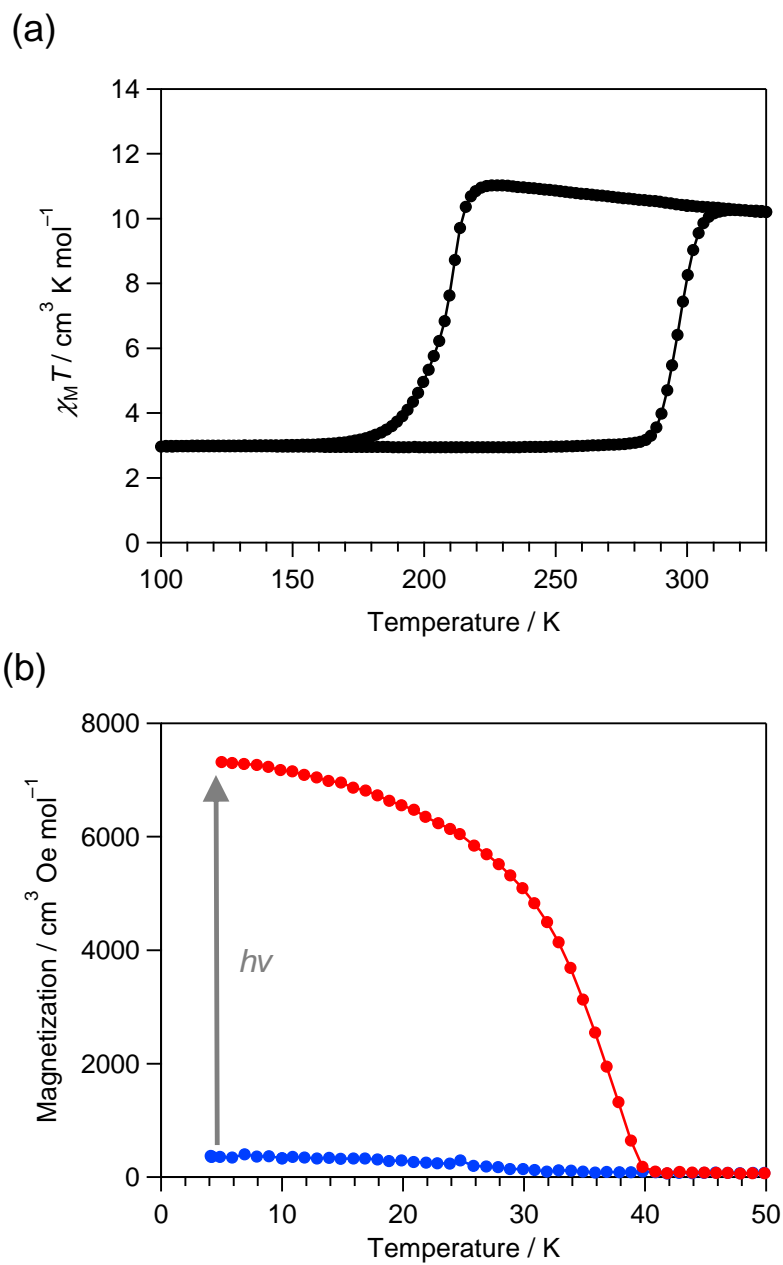


**Figure 1.14** (a) Thermal phase transition and (b) photomagnetic phenomenon of  $\text{Co}_3[\text{W}(\text{CN})_8]_2(\text{pyrimidine})_4 \cdot 6\text{H}_2\text{O}$ . Reprinted with permission from ref. 11c. Copyright 2008 American Chemical Society.

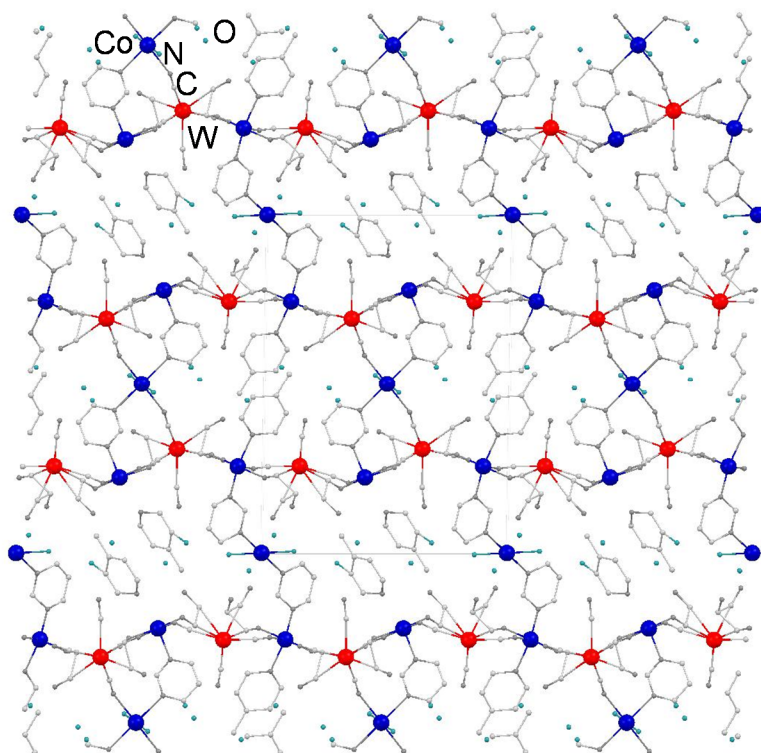


**Figure 1.15** Crystal structure of  $\text{Co}_3[\text{W}(\text{CN})_8]_2(\text{pyrimidine})_2(4\text{-methylpyridine})_2 \cdot 6\text{H}_2\text{O}$ . Reprinted with permission from ref. 11d. Copyright 2012 WILEY-VCH Verlag GmbH & Co. KGaA, Weinheim.

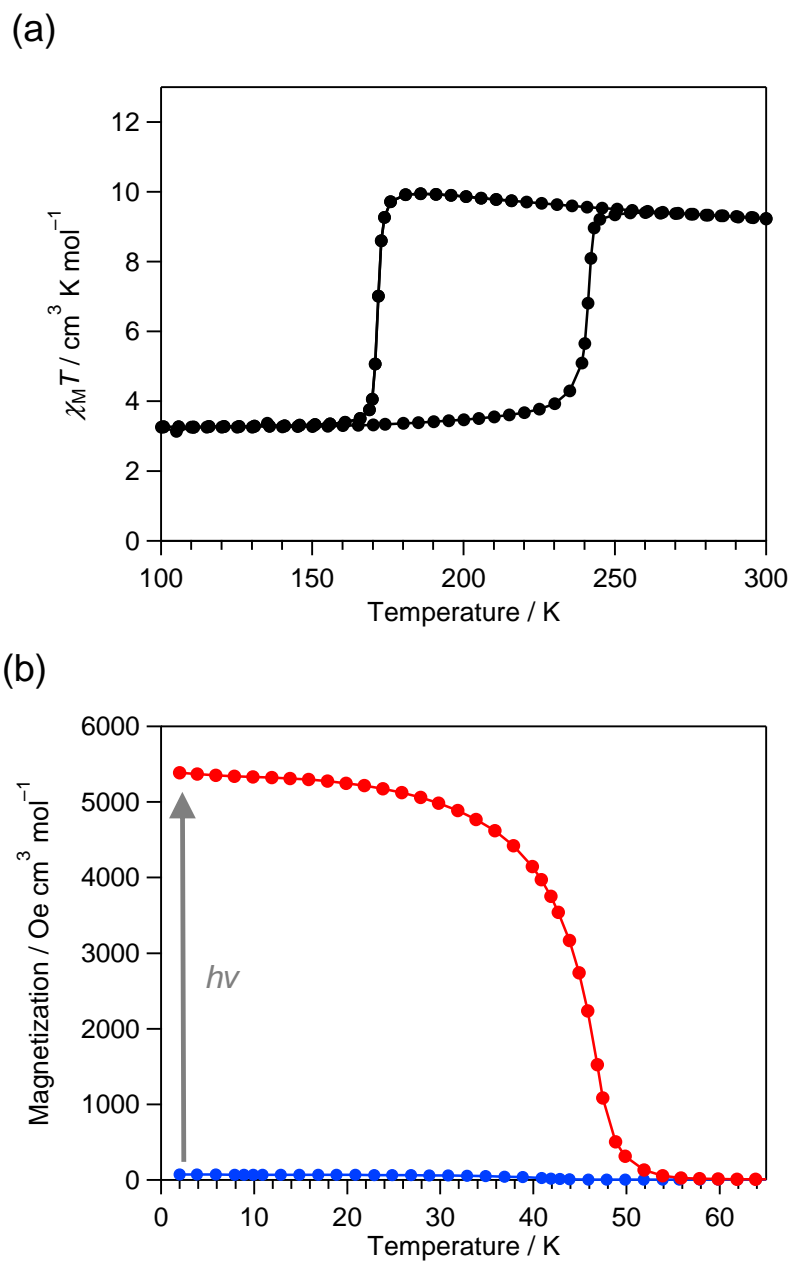


**Figure 1.16** (a) Thermal phase transition and (b) photomagnetic phenomenon of  $\text{Co}_3[\text{W}(\text{CN})_8]_2(\text{pyrimidine})_2(4\text{-methylpyridine})_2 \cdot 6\text{H}_2\text{O}$ . Reprinted with permission from ref. 11d. Copyright 2012 WILEY-VCH Verlag GmbH & Co. KGaA, Weinheim.

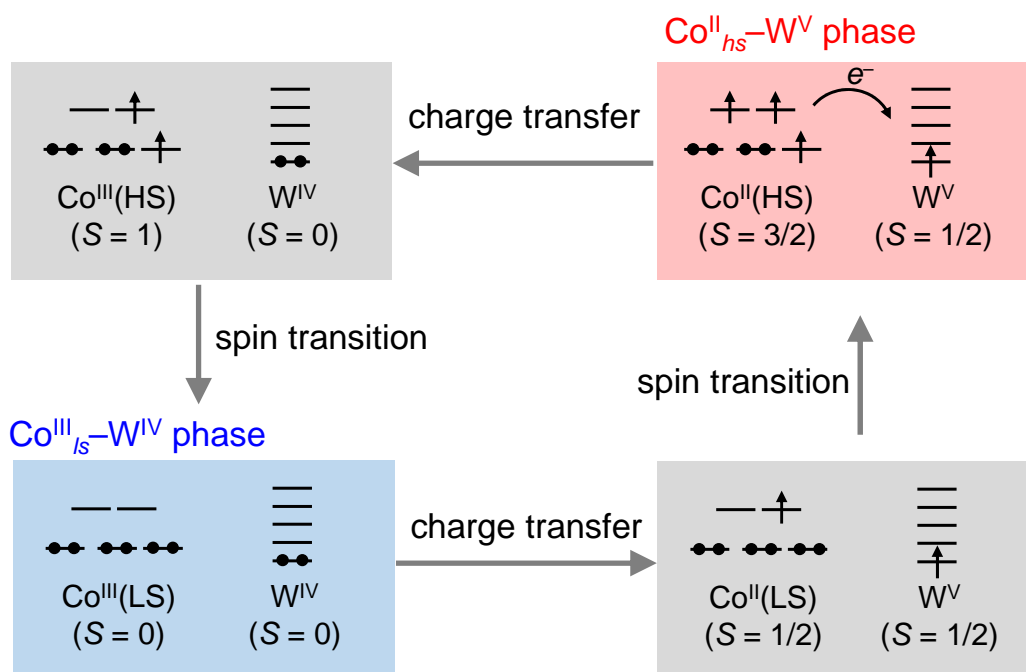


**Figure 1.17** Schematic illustration of CTIST.

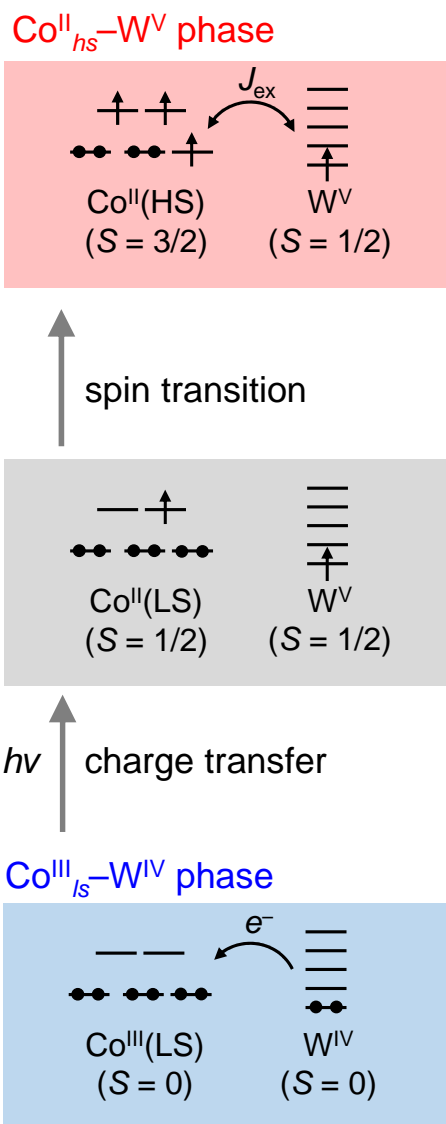


**Figure 1.18** Schematic illustration of photo-induced magnetization in a cobalt-octacyanidotungstate bimetal assembly.

## **Chapter 2**

# **Synthesis, crystal structure, and characterization of a two-dimensional cobalt–octacyanidotungstate bimetal assembly**

---

単行本もしくは雑誌掲載等の形で刊行される予定であるため、本章については、非公開



## **Chapter 3**

# **Periodic structure calculations of a two-dimensional cobalt–octacyanidotungstate bimetal assembly**

---

単行本もしくは雑誌掲載等の形で刊行される予定であるため、本章については、非公開

## **Chapter 4**

# **Photo-induced magnetization of a two-dimensional cobalt–octacyanidotungstate bimetal assembly**

---

単行本もしくは雑誌掲載等の形で刊行される予定であるため、本章については、非公開

## Chapter 5

### Summary and perspective

---

In my thesis, I focused on cobalt–octacyanidotungstate bimetal assemblies, which are photomagnets with high Curie temperatures and large coercive fields. The photomagnetism is based on photo-induced phase transition from  $\text{Co}^{\text{III}}_{ls}(S = 0)\text{--W}^{\text{IV}}(S = 0)$  to  $\text{Co}^{\text{II}}_{hs}(S = 3/2)\text{--W}^{\text{V}}(S = 1/2)$  phases, but the mechanism has not been understood in detail. An objective in my thesis is to reveal the photo-induced magnetization mechanism in cobalt–octacyanidotungstate bimetal assemblies. Periodic structure calculations are effective methods to investigate the mechanism because the calculations give electronic structure to discuss optical transitions. Detail information of a crystal structure is required to conduct the calculations. Therefore, we needed a crystal structure of the original phase of  $\text{Co}^{\text{III}}_{ls}\text{--W}^{\text{IV}}$  to understand the mechanism of the photo-induced magnetization. However, in cobalt–octacyanidotungstate bimetal assemblies, the crystal structures of the  $\text{Co}^{\text{III}}_{ls}\text{--W}^{\text{IV}}$  phase have not been determined in detail. I successfully synthesized single crystals of a cobalt–octacyanidotungstate bimetal assembly and revealed the crystal structure of the  $\text{Co}^{\text{III}}_{ls}\text{--W}^{\text{IV}}$  phase. Photo-induced magnetization of this compound was investigated from both theoretical and experimental viewpoints.

In Chapter 2, I presented the synthetic method, the crystal structure, and the electronic state of the cobalt–octacyanidotungstate bimetal assembly,  $(\text{H}_5\text{O}_2^+)[\text{Co}^{\text{III}}(4\text{-bromopyridine})_2\{\text{W}^{\text{IV}}(\text{CN})_8\}]$ . A synchrotron radiation (SR) X-ray crystal structural analysis revealed the crystal structure. This compound has a two-dimensional layer structure composed of cyanide-bridged Co and W ions. Oxonium cations  $\text{H}_5\text{O}_2^+$  are

intercalated between the layers. The electronic state was  $\text{Co}^{\text{III}}_{ls}(S = 0) - \text{W}^{\text{IV}}(S = 0)$  in the 2–390 K range even though all the previously reported cobalt–octacyanidotungstate bimetal assemblies takes  $\text{Co}^{\text{II}}_{hs}(S = 3/2) - \text{W}^{\text{V}}(S = 1/2)$  state at room temperature. The origin of stabilizing  $\text{Co}^{\text{III}}_{ls} - \text{W}^{\text{IV}}$  phase even at room temperature is the stabilization of  $\text{W}^{\text{IV}}(\text{CN})_8$  by protonation. The determined crystal structure enabled to perform periodic structure calculations to discuss optical transition in cobalt–octacyanidotungstate bimetal assemblies.

In Chapter 3, the periodic structure calculations were conducted using the crystal structure of  $(\text{H}_5\text{O}_2^+)[\text{Co}^{\text{III}}(4\text{-bromopyridine})_2\{\text{W}^{\text{IV}}(\text{CN})_8\}]$ . The calculations revealed the electronic structure of this compound. The band gap consisted of a valence band contributed from W 5d orbitals and a conduction band due to Co 3d orbitals. The calculated optical absorption spectrum reproduced well the experimental UV–vis spectrum taking the absorption band around 1.8 eV (700 nm), which was due to the charge transfer from the W valence band to the Co conduction band. The absorption of d-d transition in Co was not observed in visible region because Co valence band was below –3.5 eV. Therefore, visible light irradiation does not induce the spin transition in Co, but the charge transfer from W to Co. The calculation suggests that the mechanism of photomagnetism in cobalt–octacyanidotungstate bimetal assemblies is an optical CTIST.

In Chapter 4, considering the results of the periodic structure calculations indicating that light irradiation around 700 nm induces the charge transfer from  $\text{W}^{\text{IV}}$  to  $\text{Co}^{\text{III}}$ , I investigated photomagnetic effects in  $(\text{H}_5\text{O}_2^+)[\text{Co}(4\text{-bromopyridine})_2\{\text{W}(\text{CN})_8\}]$  by magnetic measurements, UV–vis measurements, and powder XRD measurements. In the magnetic measurements, spontaneous magnetization was observed by irradiating with 785-nm CW laser light at 3 K. The photo-induced phase exhibited ferromagnetism with

a  $T_C$  value of 27 K and an  $H_c$  value of 2000 Oe. Reversible changes by the light irradiation and annealing up to 80 K were observed. The UV–vis measurements and the crystal structural analysis suggested that the light irradiation produced the  $\text{Co}^{\text{II}}\text{--W}^{\text{V}}$  state. The photomagnetism can be explained by optical CTIST in the light of the results of the calculations and the light irradiation experiments. This is the first example to determine the crystal structure of the photo-induced phase in cobalt–octacyanidotungstate bimetal assemblies.

As mentioned above, I successfully obtained the stabilized  $\text{Co}^{\text{III}}\text{--W}^{\text{IV}}$  phase even at room temperature by protonating  $\text{W}^{\text{IV}}(\text{CN})_8$  in the crystal structure, indicating that including proton in crystal structures of materials showing charge transfer phase transition can dramatically change the phase transition temperature. The periodic structure calculations showed the electronic structure to enable us to discuss the photo-induced mechanism. As we are also able to obtain information about effects of organic ligands to electronic structure, the results of the calculations lead to design metal complexes exhibiting photo-induced phase transition and photo-induced magnetization. Additionally, I determined the crystal structure of the photo-induced phase, giving more information about the photo-induced magnetization such as magnetic interaction and magnetic anisotropy. Therefore, the determination of the crystal structure is important to contrive photomagnets. These results in my thesis give guideline to design phase transition materials and photomagnets are expected to develop these study fields.

## References

---

- 1 (a) M. L. Plumer, J. van Ek, D. Weller, *The Physics of Ultra-High Density Magnetic Recording*, Springer, Berlin, **2001**.  
(b) Y. Nakamura, *Advanced Technologies of Perpendicular Magnetic Recording*, CMC Publishing, Tokyo, **2007**.  
(c) T. Hayashi, S. Hirono, M. Tomita, S. Umemura, *Nature* **1996**, *381*, 772.  
(d) D. Weller, A. Moser, *IEEE Trans. Magn.* **1999**, *35*, 4423.  
(e) S. Ohkoshi, A. Namai, K. Imoto, M. Yoshikiyo, W. Tarora, K. Nakagawa, M. Komine, Y. Miyamoto, T. Nasu, S. Oka, H. Tokoro, *Sci. Rep.* **2015**, *5*, 14414.  
(f) S. Ohkoshi, A. Namai, M. Yoshikiyo, K. Imoto, K. Tamasaki, K. Matsuno, O. Inoue, T. Ide, K. Masada, M. Goto, T. Goto, T. Yoshida, T. Miyazaki, *Angew. Chem. Int. Ed.* **2016**, *55*, 11403.
- 2 (a) J. F. Herbst, *Rev. Mod. Phys.* **1991**, *63*, 819.  
(b) E. Burzo, *Rep. Prog. Phys.* **1998**, *61*, 1099.
- 3 (a) S. Ohkoshi, S. Kuroki, S. Sakurai, K. Matsumoto, K. Sato, S. Sasaki, *Angew. Chem. Int. Ed.* **2007**, *46*, 8392.  
(b) A. Namai, M. Yoshikiyo, K. Yamada, S. Sakurai, T. Goto, T. Yoshida, T. Miyazaki, M. Nakajima, T. Suemoto, H. Tokoro, S. Ohkoshi, *Nature Commun.* **2012**, *3*, 1035.
- 4 (a) H. H. Wickman, A. M. Trozzolo, H. J. Williams, G. W. Hull, F. R. Merritt, *Phys. Rev.* **1967**, *155*, 563.  
(b) Y. Pei, M. Verdaguer, O. Kahn, *J. Am. Chem. Soc.* **1986**, *108*, 7428.  
(c) J. S. Miller, J. C. Calabrese, H. Rommelmann, S. R. Chittipeddi, J. H. Zhang, W. M. Reiff, A. J. Epstein, *J. Am. Chem. Soc.* **1987**, *109*, 769.  
(d) A. Caneschi, D. Gatteschi, J. P. Renard, P. Rey, R. Sessoli, *J. Am. Chem. Soc.* **1989**, *111*, 785.
- 5 (a) O. Sato, T. Iyoda, A. Fujishima, K. Hashimoto, *Science* **1996**, *272*, 704.  
(b) N. Simamoto, S. Ohkoshi, O. Sato, K. Hashimoto, *Inorg. Chem.* **2002**, *41*, 678.  
(c) O. Sato, S. Hayami, Y. Einaga, Z.-Z. Gu, *Bull. Chem. Soc. Jpn.* **2003**, *76*, 443.

- 6 (a) S. Ohkoshi, S. Yorozu, O. Sato, T. Iyoda, A. Fujishima, K. Hashimoto, *Appl. Phys. Lett.* **1997**, *70*, 1040.  
(b) S. Ohkoshi, K. Hashimoto, *J. Am. Chem. Soc.* **1999**, *121*, 10591.
- 7 (a) H. Tokoro, T. Matsuda, T. Nuida, Y. Moritomo, K. Ohoyama, E. D. L. Dangui, K. Boukheddaden, S. Ohkoshi, *Chem. Mater.* **2008**, *20*, 423.  
(b) H. Tokoro, S. Ohkoshi, *Bull. Chem. Soc. Jpn.* **2015**, *88*, 227.
- 8 (a) D. M. Pajerowski, M. J. Andrus, J. E. Gardner, E. S. Knowles, M. W. Meisel, D. R. Talham, *J. Am. Chem. Soc.* **2010**, *132*, 4058.  
(b) O. N. Risset, P. A. Quintero, T. V. Brinzari, M. J. Andrus, M. W. Lufaso, M. W. Meisel, D. R. Talham, *J. Am. Chem. Soc.* **2014**, *136*, 15660.
- 9 S. Ohkoshi, H. Tokoro, *Acc. Chem. Res.* **2012**, *45*, 1749.
- 10 (a) T. Hozumi, K. Hashimoto, S. Ohkoshi, *J. Am. Chem. Soc.* **2005**, *127*, 3864.  
(b) S. Ohkoshi, H. Tokoro, T. Hozumi, Y. Zhang, K. Hashimoto, C. Mathoniere, I. Bord, G. Rombaut, M. Verelst, C. C. D. Moulin, F. Villain, *J. Am. Chem. Soc.* **2006**, *128*, 270.  
(c) H. Tokoro, K. Nakagawa, K. Nakabayashi, T. Kashiwagi, K. Hashimoto, S. Ohkoshi, *Chem. Lett.* **2009**, *38*, 338.  
(d) Y. Umetsu, S. Chorazy, K. Nakabayashi, S. Ohkoshi, *Euro. J. Inorg. Chem.* **2016**, 1980.
- 11 (a) Y. Arimoto, S. Ohkoshi, Z. J. Zhong, H. Seino, Y. Mizobe, K. Hashimoto, *J. Am. Chem. Soc.* **2003**, *125*, 9240.  
(b) R. Le Bris, C. Mathonière, J. F. Létard, *Chem. Phys. Lett.* **2006**, *426*, 380.  
(c) S. Ohkoshi, S. Ikeda, T. Hozumi, T. Kashiwagi, K. Hashimoto, *J. Am. Chem. Soc.* **2006**, *128*, 5320.  
(d) S. Ohkoshi, Y. Hamada, T. Matsuda, Y. Tsunobuchi, H. Tokoro, *Chem. Mater.* **2008**, *20*, 3048.  
(e) N. Ozaki, H. Tokoro, Y. Hamada, A. Namai, T. Matsuda, S. Kaneko, S. Ohkoshi, *Adv. Funct. Mater.* **2012**, *22*, 2089.  
(f) R. L. Bris, Y. Tsunobuchi, C. Mathonière, H. Tokoro, S. Ohkoshi, N. Ould-Moussa, G. Molnar, A. Bousseksou, J. F. Létard, *Inorg. Chem.* **2012**, *51*, 2852.
- 12 (a) S. Ohkoshi, K. Imoto, Y. Tsunobuchi, S. Takano, H. Tokoro, *Nature Chem.* **2011**, *3*, 564.

- (b) S. Ohkoshi, S. Takano, K. Imoto, M. Yoshikiyo, A. Namai, H. Tokoro, *Nature Photonics* **2014**, *8*, 65.
- (c) D. Pinkowicz, M. Rams, M. Mišek, K. V. Kamenev, H. Tomkowiak, A. Katrusiak, B. Sieklucka, *J. Am. Chem. Soc.* **2015**, *137*, 8795.
- (d) K. Imoto, S. Ohkoshi, *Chem. Lett.* **2016**, *45*, 359.
- 13 (a) S. Ohkoshi, K. Arai, Y. Sato, K. Hashimoto, *Nature Mater.* **2004**, *3*, 857.
- (b) K. Imoto, D. Takahashi, Y. Tsunobuchi, M. Arai, W. Kosaka, H. Tokoro, S. Ohkoshi, *Eur. J. Inorg. Chem.* **2010**, 4079.
- (c) H. Tokoro, S. Ohkoshi, *Curr. Inorg. Chem.* **2014**, *4*, 100.
- 14 S. Ohkoshi, Y. Tsunobuchi, H. Takahashi, T. Hozumi, M. Shiro, K. Hashimoto, *J. Am. Chem. Soc.* **2007**, *129*, 3084.
- 15 (a) K. K. Orisaku, K. Nakabayashi, S. Ohkoshi, *Chem. Lett.* **2011**, *40*, 586.
- (b) K. K. Orisaku, K. Imoto, Y. Koide, S. Ohkoshi, *Cryst. Growth Des.* **2013**, *13*, 5267.
- 16 S. Ohkoshi, H. Tokoro, T. Matsuda, H. Takahashi, H. Irie, K. Hashimoto, *Angew. Chem. Int. Ed.* **2007**, *46*, 3238.
- 17 (a) S. Ohkoshi, K. Nakagawa, K. Tomono, K. Imoto, Y. Tsunobuchi, H. Tokoro, *J. Am. Chem. Soc.* **2010**, *132*, 6620.
- (b) E. Pardo, C. Train, G. Gontard, K. Boubekeur, O. Fabelo, H. Liu, B. Dkhil, F. Lloret, K. Nakagawa, H. Tokoro, S. Ohkoshi, M. Verdager, *J. Am. Chem. Soc.* **2011**, *133*, 15328.
- (c) K. Imoto, K. Nakagawa, H. Miyahara, S. Ohkoshi, *Cryst. Growth Des.* **2013**, *13*, 4673.
- (d) C. Maxim, S. Ferlay, H. Tokoro, S. Ohkoshi, C. Train, *Chem. Commun.* **2014**, *50*, 5629.
- 18 (a) K. Ikeda, S. Ohkoshi, K. Hashimoto, *J. Appl. Phys.* **2003**, *93*, 1371.
- (b) T. Nuida, T. Matsuda, H. Tokoro, S. Sakurai, K. Hashimoto, S. Ohkoshi, *J. Am. Chem. Soc.* **2005**, *127*, 11604.
- (c) S. Ohkoshi, J. Shimura, K. Ikeda, K. Hashimoto, *J. Opt. Soc. Am. B* **2005**, *22*, 196.
- (d) Y. Tsunobuchi, W. Kosaka, T. Nuida, S. Ohkoshi, *CrystEngComm* **2009**, *11*, 2051.



- (e) C. Train, T. Nuida, R. Gheorghe, M. Gruselle, S. Ohkoshi, *J. Am. Chem. Soc.* **2009**, *131*, 16838.
- (f) D. Pinkowicz, R. Podgajny, W. Nitek, M. Rams, A. M. Majcher, T. Nuida, S. Ohkoshi, B. Sieklucka, *Chem. Mater.* **2011**, *23*, 21.
- 19 S. Chikazumi, *Physics of Magnetism*, Wiley, New York, **1964**.
- 20 (a) M. Verdaguer, A. Bleuzen, V. Marvaud, J. Vaissermann, M. Seuleiman, C. Desplanches, A. Sculler, C. Train, R. Garde, G. Gelly, C. Lomenech, I. Rosenman, P. Veillet, C. Cartier, F. Villain, *Coord. Chem. Rev.* **1999**, *190*, 1023.
- (b) B. Sieklucka, R. Podgajny, T. Korzeniak, P. Przychodzeń, R. Kania, *C. R. Chim.* **2002**, *5*, 639.
- (c) P. Przychodzeń, T. Korzeniak, R. Podgajny, B. Sieklucka, *Coord. Chem. Rev.* **2006**, *250*, 2234.
- (d) B. Sieklucka, R. Podgajny, D. Pinkowicz, B. Nowicka, T. Korzeniak, M. Bałanda, T. Wasiutyński, R. Pełka, M. Makarewicz, M. Czaplą, M. Rams, B. Gawęł, W. Łasocha, *CrystEngComm* **2009**, *11*, 2032.
- (e) B. Sieklucka, R. Podgajny, T. Korzeniak, B. Nowicka, D. Pinkowicz, M. Koziel, *Eur. J. Inorg. Chem.* **2011**, *3*, 305.
- (f) D. Pinkowicz, R. Podgajny, B. Nowicka, S. Chorazy, M. Reczyński, B. Sieklucka, *Inorg. Chem. Front.* **2015**, *2*, 10.
- 21 S. Ferlay, T. Mallah, R. Ouahés, P. Veillet, M. Verdaguer, *Nature* **1995**, *387*, 701.
- 22 (a) S. Ohkoshi, T. Iyoda, *Phys. Rev. B* **1997**, *56*, 11642.
- (b) S. Ohkoshi, K. Hashimoto, *Phys. Rev. B* **1999**, *60*, 12820.
- 23 S. Ohkoshi, Y. Abe, A. Fujishima, K. Hashimoto, *Phys. Rev. Lett.* **1999**, *82*, 1285.
- 24 (a) T. Matsuda, H. Tokoro, K. Hashimoto, S. Ohkoshi, *Dalton Trans.* **2006**, 5046.
- (b) H. Tokoro, K. Nakagawa, K. Imoto, F. Hakoe, S. Ohkoshi, *Chem. Mater.* **2012**, *24*, 1324.
- 25 A. Takahashi, H. Tanaka, D. Parajuli, T. Nakamura, K. Minami, Y. Sugiyama, Y. Hakuta, S. Ohkoshi, T. Kawamoto, *J. Am. Chem. Soc.* **2016**, *138*, 6376.
- 26 (a) J. K. Burdett, R. Hoffmann, R. C. Fay, *Inorg. Chem.* **1978**, *17*, 2553.
- (b) B. Sieklucka, R. Podgajny, P. Przychodzeń, T. Korzeniak, *Coord. Chem. Rev.* **2005**, *249*, 2203.
- 27 (a) R. Podgajny, C. Desplanches, B. Sieklucka, R. Sessoli, V. Villar, C. Paulsen, W.

- Wernsdorfer, Y. Dromzée, M. Verdaguer, *Inorg. Chem.* **2002**, *41*, 1323.
- (b) Z. J. Zhong, H. Seino, Y. Mizobe, M. Hidai, A. Fujishima, S. Ohkoshi, K. Hashimoto, *J. Am. Chem. Soc.* **2000**, *122*, 2952.
- (c) J. M. Herrera, V. Marvaud, M. Verdaguer, J. Marrot, M. Kalisz, C. Mathonière, *Angew. Chem. Int. Ed.* **2004**, *43*, 5468.
- (d) Y. Song, P. Zhang, X.-M. Ren, X.-F. Shen, Y.-Z. Li, X.-Z. You, *J. Am. Chem. Soc.* **2005**, *127*, 3708.
- (e) J. H. Lim, J. H. Yoon, H. C. Kim, C. S. Hong, *Angew. Chem. Int. Ed.* **2006**, *45*, 7424.
- (f) D. E. Freedman, M. V. Bennett, J. R. Long, *Dalton Trans.* **2006**, *23*, 2829.
- (g) S. Chorazy, R. Podgajny, W. Nogaś, W. Nitek, M. Kozieł, M. Rams, E. Juszyńska, J. Żukrowski, C. Kapusta, K. Nakabayashi, T. Fujimoto, S. Ohkoshi, B. Sieklucka, *Chem. Commun.* **2014**, *50*, 3484.
- (h) S. Chorazy, R. Podgajny, K. Nakabayashi, J. Stanek, M. Rams, B. Sieklucka, S. Ohkoshi, *Angew. Chem. Int. Ed.* **2015**, *54*, 5093.
- (i) S. Chorazy, J. Stanek, W. Nogas, A. Majcher, M. Rams, M. Kozieł, E. Juszyńska-Gałązka, K. Nakabayashi, S. Ohkoshi, B. Sieklucka, R. Podgajny, *J. Am. Chem. Soc.* **2016**, *138*, 1635.
- 28 (a) G. Rombaut, S. Golhen, L. Ouahab, C. Mathonière, O. Kahn, *J. Chem. Soc., Dalton Trans.* **2000**, 3609.
- (b) R. Pradhan, C. Desplanches, P. Guionneau, J.-P. Sutter, *Inorg. Chem.* **2003**, *42*, 6607.
- (c) D. Li, L. Zheng, Y. Zhang, J. Huang, S. Gao, W. Tang, *Inorg. Chem.* **2003**, *42*, 6123.
- (d) S. Ikeda, T. Hozumi, K. Hashimoto, S. Ohkoshi, *Dalton Trans.* **2005**, 2120.
- (e) P. Przychodzeń, K. Lewiński, R. Pelka, M. Balanda, K. Tomala, B. Sieklucka, *Dalton Trans.* **2006**, 625.
- (f) F. Prins, E. Pasca, L. J. Jongh, H. Kooijman, A. L. Spek, S. Tanase, *Angew. Chem. Int. Ed.* **2007**, *46*, 6081.
- 29 (a) R. Podgajny, T. Korzeniak, M. Balanda, T. Wasiutynski, W. Errington, T. J. Kemp, N. W. Alcock, B. Sieklucka, *Chem. Commun.* **2002**, 1138.
- (b) T. Hozumi, S. Ohkoshi, Y. Arimoto, H. Seino, Y. Mizobe, K. Hashimoto, *J.*

- Phys. Chem. B* **2003**, *107*, 11571.
- (c) J. Larionova, R. Clérac, B. Donnadiou, S. Willemin, C. Guérin, *Cryst. Growth Des.* **2003**, *3*, 267.
- (d) S. Kaneko, Y. Tsunobuchi, S. Sakurai, S. Ohkoshi, *Chem. Phys. Lett.* **2007**, *446*, 292.
- (e) D. Takahashi, K. Nakabayashi, S. Tanaka, S. Ohkoshi, *Inorg. Chem. Commun.* **2013**, *27*, 47.
- 30 (a) R. Garde, C. Desplanches, A. Bleuzen, P. Veillet, M. Verdaguer, *Mol. Cryst. Liq. Cryst.* **1999**, *334*, 587.
- (b) Z. J. Zhong, H. Seino, Y. Mizobe, M. Hidai, M. Verdaguer, S. Ohkoshi, K. Hashimoto, *Inorg. Chem.* **2000**, *39*, 5095.
- (c) J. M. Herrera, A. Bleuzen, Y. Dromzée, M. Julve, F. Lloret, M. Verdaguer, *Inorg. Chem.* **2003**, *42*, 7052.
- (d) T. Kashiwagi, S. Ohkoshi, H. Seino, Y. Mizobe, K. Hashimoto, *J. Am. Chem. Soc.* **2004**, *126*, 5024.
- (e) J. M. Herrera, P. Franz, R. Podgajny, M. Pilkington, M. Biner, S. Decurtins, H. Stoeckli-Evans, A. Neels, R. Garde, Y. Dromzée, M. Julve, B. Sieklucka, K. Hashimoto, S. Ohkoshi, M. Verdaguer, *C. R. Chim.* **2008**, *11*, 1192.
- (f) K. Imoto, M. Takemura, K. Nakabayashi, Y. Miyamoto, K. K. Orisaku, S. Ohkoshi, *Inorg. Chim. Acta* **2015**, *425*, 92.
- 31 K. Imoto, M. Takemura, H. Tokoro, S. Ohkoshi, *Eur. J. Inorg. Chem.* **2012**, 2649.
32. (a) Y. Tsunobuchi, S. Kaneko, K. Nakabayashi, S. Ohkoshi, *Cryst. Growth Des.* **2011**, *11*, 5561.
- (b) K. Nakabayashi, S. Chorazy, D. Takahashi, T. Kinoshita, B. Sieklucka, S. Ohkoshi, *Cryst. Growth Des.* **2014**, *14*, 6093.
- (c) K. Nakabayashi, S. Chorazy, Y. Miyamoto, T. Fujimoto, K. Yazawa, D. Takahashi, B. Sieklucka, S. Ohkoshi, *CrystEngComm* **2016**, *18*, 9236.
- 33 (a) S. Chorazy, K. Nakabayashi, N. Ozaki, R. Peřka, T. Fic, J. Mlynarski, B. Sieklucka, S. Ohkoshi, *RSC Adv.* **2013**, *3*, 1065.
- (b) S. Chorazy, K. Nakabayashi, S. Ohkoshi, B. Sieklucka, *Chem. Mater.* **2014**, *26*, 4072.
- (c) S. Chorazy, K. Nakabayashi, M. Arczynski, R. Peřka, S. Ohkoshi, B. Sieklucka,

- Chem. Eur. J.* **2014**, *20*, 7144.
- (d) S. Chorazy, M. Arczynski, K. Nakabayashi, B. Sieklucka, S. Ohkoshi, *Inorg. Chem.* **2015**, *54*, 4724.
- (e) S. Chorazy, B. Sieklucka, S. Ohkoshi, *Cryst. Growth Des.* **2016**, *16*, 4918 (2016).
- (f) S. Chorazy, J. Wang, S. Ohkoshi, *Chem. Commun.* **2016**, *52*, 10795.
34. (a) K. Nasu, *Relaxations of Excited States and Photo-Induced Structural Phase Transitions*, Springer-Verlag, Berlin, **1997**.
- (b) K. Nasu, *Rep. Prog. Phys.* **2004**, *67*, 1607.
35. (a) E. R. Meinders, A. V. Mijrskii, L. van Pieteron, M. Wuttig, *Optical Data Storage: Phase Change Media and Recording*, Springer, Berlin, **2006**.
- (b) O.Kahn, C. J. Martinez, *Science* **1998**, *279*, 44.
- (c) P. Gütllich, A. Hauser, H. Spiering, *Angew. Chem. Int. Ed. Engl.* **1994**, *33*, 2024.
- (d) S. Bonhommeau, G. Molnár, A. Galet, A. Zwick, J. A. Real, J. J. McGarvey, A. Bousseksou, *Angew. Chem. Int. Ed.* **2005**, *44*, 4069.
- (e) A. Dei, *Angew. Chem. Int. Ed.* **2005**, *44*, 1160.
- (f) A. Bleuzen, V. Marvaud, C. Mathonière, B. Sieklucka, M. Verdaguer, *Inorg. Chem.* **2009**, *48*, 3453.
36. (a) N. Yamada, E. Ohno, K. Nishiuchi, N. Akahira, M. Takao, *J. Appl. Phys.* **1991**, *69*, 2849.
- (b) A. V. Kolobov, P. Fons, A. I. Frenkel, A. L. Ankudinov, J. Tominaga, T. Uruga, *Nature Mater.* **2004**, *3*, 703.
- (c) M. Wuttig, N. Yamada, *Nature Mater.* **2007**, *6*, 824.
37. (a) M. Fiebig, K. Miyano, Y. Tomioka, Y. Tokura, *Science* **1998**, *280*, 1925.
- (b) S. Ohkoshi, Y. Tsunobuchi, T. Matsuda, K. Hashimoto, A. Namai, F. Hakoe, H. Tokoro, *Nature Chem.* **2010**, *2*, 539.
- (c) H. Tokoro, M. Yoshikiyo, K. Imoto, A. Namai, T. Nasu, K. Nakagawa, N. Ozaki, F. Hakoe, K. Tanaka, K. Chiba, R. Makiura, K. Prassides, S. Ohkoshi, *Nature Commun.* **2015**, *6*, 7037.
38. (a) S. Decurtins, P. Gütllich, C. P. Köhler, H. Spiering, A. Hauser, *Chem. Phys. Lett.* **1984**, *105*, 1.
- (b) J. F. Létard, P. Guionneau, E. Codjovi, O. Lavastre, G. Bravic, D. Chasseau, O. Kahn, *J. Am. Chem. Soc.* **1997**, *119*, 10861.

- (c) F. Renz, H. Ohshio, V. Ksenofontov, M. Waldeck, H. Spiering, P. Gütllich, *Angew. Chem. Int. Ed.* **2000**, *39*, 3699.
- (d) S. Cobo, D. Ostrovskii, S. Bonhommeau, L. Vendier, G. Molnar, L. Salmon, K. Tanaka, A. Bousseksou, *J. Am. Chem. Soc.* **2008**, *130*, 9019.
- (e) M. Clemente-León, E. Coronado, M. López-Jordá, C. Desplanches, S. Asthana, H. Wangb, J.-F. Létard, *Chem. Sci.* **2011**, *2*, 1121.
- (f) N. F. Sciortino, K. R. Scherl-Gruenwald, G. Chastanet, G. J. Halder, K. W. Chapman, J.-F. Létard, C. J. Kepert, *Angew. Chem. Int. Ed.* **2012**, *51*, 10154.
- (g) K. D. Murnaghan, C. Carbonera, L. Toupet, M. Griffin, M. M. Dîrtu, C. Desplanches, Y. Garcia, E. Collet, J.-F. Létard, G. G. Morgan, *Chem. Eur. J.* **2014**, *20*, 5613.
- (h) R. Bertoni, M. Cammarata, M. Lorenc, S. Matar, J. F. Létard, H. Lemke, E. Collet, *Acc. Chem. Res.* **2015**, *48*, 774.
- 39 (a) N. Shimamoto, S. Ohkoshi, O. Sato, K. Hashimoto, *Chem. Lett.* **2002**, *4*, 486.
- (b) H. Tokoro, T. Matsuda, K. Hashimoto, S. Ohkoshi, *J. Appl. Phys.* **2005**, *97*, 10M508.
- (c) H. Tokoro, S. Ohkoshi, *Appl. Phys. Lett.* **2008**, *93*, 021906.
- (d) A. Bleuzen, V. Marvaud, C. Mathoniere, B. Sieklucka, M. Verdaguer, *Inorg. Chem.* **2009**, *48*, 3453.
- (e) C. Avendano, M. G. Hilfiger, A. Prosvirin, C. Sanders, D. Stepien, K. R. Dunbar, *J. Am. Chem. Soc.* **2010**, *132*, 13123.
- (f) K. E. Funck, A. V. Prosvirin, C. Mathonière, R. Clérac, K. R. Dunbar, *Inorg. Chem.* **2011**, *50*, 2782.
- (g) E. S. Koumoussi, I.-R. Jeon, Q. Gao, P. Dechambenoit, D. N. Woodruff, P. Merzeau, L. Buisson, X. Jia, D. Li, F. Volatron, C. Mathonière, C. Clérac, *J. Am. Chem. Soc.* **2014**, *136*, 15461.
- (h) Y.-Z. Zhang, P. Ferko, D. Siretanu, R. Ababei, N. P. Rath, M. J. Shaw, R. Clérac, C. Mathonière, S. M. Holmes, *J. Am. Chem. Soc.* **2014**, *136*, 16854.
- 40 (a) S. Chorazy, K. Nakabayashi, K. Imoto, J. Mlynarski, B. Sieklucka, S. Ohkoshi *J. Am. Chem. Soc.* **2012**, *134*, 16151.
- (b) S. Chorazy, R. Podgajny, W. Nitek, M. Rams, S. Ohkoshi, B. Sieklucka, *Cryst. Growth Des.* **2013**, *13*, 3036.

- (c) S. Chorazy, M. Reczynski, R. Podgajny, W. Nogas, S. Buda, M. Rams, W. Nitek, B. Nowicka, J. Mlynarski, S. Ohkoshi, B. Sieklucka, *Cryst. Growth Des.* **2015**, *15*, 3573.
- (d) S. Chorazy, A. Hoczek, M. Kubicki, H. Tokoro, S. Ohkoshi, B. Sieklucka, R. Podgajny, *CrystEngComm* **2016**, *18*, 1495.
- (e) S. Chorazy, M. Rams, A. Hoczek, B. Czarnecki, B. Sieklucka, S. Ohkoshi, R. Podgajny, *Chem. Commun.* **2016**, *52*, 4772.
- 41 (a) J. G. Leipoldt, L. D. C. Bok, P. J. Cilliers, *Z. Anorg. Allg. Chem.* **1974**, *407*, 350.  
(b) L. D. C. Bok, J. G. Leipoldt, S. S. Basson, *Z. Anorg. Allg. Chem.* **1975**, *415*, 81.  
(c) L. D. C. Bok, J. G. Leipoldt, S. S. Basson, *Acta Crystallogr. Sect. B* **1970**, *26*, 684.
- 42 G. M. Sheldrick, *Acta Cryst. A* **2008**, *64*, 112.
- 43 E. S. Stoyanov, C. A. Reed, *J. Phys. Chem. A* **2006**, *110*, 12992.
- 44 I.-R. Jeon, S. Calancea, A. Panja, D. M. P. Cruz, E. S. Koumoussi, P. Dechambenoit, C. Coulon, A. Wattiaux, P. Rosa, C. Mathonière, R. Clérac, *Chem. Sci.* **2013**, *4*, 2463.
- 45 (a) G. Kresse, J. Hafner, *Phys. Rev. B* **1993**, *47*, 558.  
(b) G. Kresse, J. Hafner, *Phys. Rev. B* **1994**, *49*, 14251.  
(c) G. Kresse, J. Furthmüller, *Comput. Mater. Sci.* **1996**, *6*, 15.  
(d) G. Kresse, J. Furthmüller, *Phys. Rev. B* **1996**, *54*, 11169.
- 46 (a) J. P. Perdew, K. Burke, M. Ernzerhof, *Phys. Rev. Lett.* **1996**, *77*, 3865.  
(b) J. P. Perdew, K. Burke, M. Ernzerhof, *Phys. Rev. Lett.* **1997**, *78*, 1396.
- 47 K. Monma, F. Izumi, *J. Appl. Crystallogr.* **2011**, *44*, 1272.
- 48 F. Izumi, K. Momma, *Solid State Phenom.* **2007**, *130*, 15.
- 49 T. S. Venkatakrisnan, I. Imaz, J.-P. Sutter, *Inorg. Chim. Acta* **2008**, *361*, 3710.

## List of paper related to the thesis

---

(1) “Photo-induced magnetization and first-principles calculations of a two-dimensional cyanide-bridged Co–W bimetal assembly”

Y. Miyamoto, T. Nasu, N. Ozaki, Y. Umeta, H. Tokoro, K. Nakabayashi, S. Ohkoshi,  
*Dalton Transactions*, 2016, 45, 19249–19256. (Inside Cover)

This paper corresponds to Chapter 2, 3, and 4.

## Acknowledgements

---

I am deeply grateful to my supervisor, Prof. Shin-ichi Ohkoshi. He gave me interesting themes and experimental environment. I am impressed by his passion and attitude to researches. I would like to thank him for giving me opportunities to participate in domestic and international conferences.

I would like to express my gratitude to Dr. Hiroko Tokoro. She gave me many advices on my research. I would like to offer my special thanks to Dr. Koji Nakabayashi. He gave me constructive comments and warm encouragement. I would like to express my gratitude to Dr. Kenta Imoto. He advised me on experiments and told me how to use experimental equipment. I thank Dr. Asuka Namai, Dr. Kosuke Nakagawa, Dr. Szymon Choraży, and Ms. Marie Yoshikiyo for helping me in many aspects of my study.

I would like to express my gratitude to senior members of Ohkoshi Laboratory, Dr. Noriaki Ozaki, Dr. Yoshikazu Umeta, and Dr. Akira Takahashi. Advice and comments given by them has been great help in my thesis.

I am grateful to my colleague of Ohkoshi Laboratory, Mr. Tomomichi Nasu. Without his help on first-principles calculations, my thesis would not have been possible.

I would like to thank all the members of Ohkoshi Laboratory, Dr. Keiko Komori-Orisaku, Ms. Shoko Ishii, Ms. Hiroko Sakuradani, Mr. Masaya Komine, Mr. Mateusz Reczyński, Mr. Takuro Ohno, Mr. Koki Shiraishi, Mr. Takanobu Taniguchi, Mr. Koichi Nakaono, Mr. Yuta Maeno, Mr. Koreyoshi Ogata, Mr. Shintaro Kawabata, Mr. Junhao Wang, Ms. Rina Kinugawa, Mr. Yuya Shibata, Mr. Seiya Tsukamoto, Mr. Satoru Honda, and Mr. Takaya Yoshida.

I am also grateful to all the members of Tokoro Laboratory, Mr. Takuya Matsunaga,



Mr. Iori Nagata, Mr. Junpei Fukui, Mr. Rei Fujiwara, Mr. Hiroki Oshiro, and Ms. Kanae Saitou. Their attitude to research encouraged me greatly.

I would like to thank Japan Society for the Promotion of Science through Program for Leading Graduate Schools (MERIT) for supporting me. I am grateful to my vice-supervisor in MERIT program, Prof. Hiroshi Okamoto for significant discussion and support. I would like to show my appreciation to the member of Okamoto Laboratory, Mr. Tsubasa Terashige for experiments and discussion of time-resolved spectroscopy.

I am grateful to Dr. Aiko Kamitsubo in the microanalytical laboratory at department of chemistry, school of science, the University of Tokyo for elemental analyses using standard microanalytical methods and ion chromatography after treatment by oxygen flask combustion.

Finally, I would like to thank my grandmother, father, mother, and brothers for their support and encouragement.

December, 2016

Yasuto Miyamoto